発表した成果（発表題目、口頭・ポスター発表の別）	発表者氏名	発表した場所（学会等名）	発表した時期	国内・外の別
Characterization of crohn disease in X-linked inhibitor of apoptosis protein-deficient male patients and female symptomatic carriers.	Aguilar C, Lenoir C, Lambert N, Begue B, Brousse N, Canioni D, Berrebi D, Roy M, Gerart S, Chapel H, Schwerd T, Siproudhis L, Schappi M, Al-Ahmari A, Yamaide A, Mori M, Galicier L, Neven B, Routes J, Ulhig H, Koletzko S, Patel S, Kanegane H, Picard C, Fischer A, Cerf Bensussan N, Ruemmele F, Hugot J.P, Latour S	16th Biennial Meeting of the European Society of Immunodeficiencies	2014年10月29日-11月1日	国外
Inflammatory bowel disease in Japanese patients with XIAP deficiency.	Nishida N, Yang X, Hoshino A, Kanegane H	16th Biennial Meeting of the European Society of Immunodeficiencies	2014年10月29日-11月1日	国外
Safety and tolerability of hizentra in patients with primary immunodeficiency in Japan, Europe and the US	Kanegane H, Imai K, Yamada M, Takada H, Ariga T, Hara T, Rojavin M, Hu W, Hubsch A, Nonoyama S	16th Biennial Meeting of the European Society of Immunodeficiencies	2014年10月29日-11月1日	国外
Clinical and immunological features of patients with Gain-of-Function PIK3CD mutations in Japan	Takashima T, Tsujita Y, Yeh T.W, Mitsuiki N, Kanegane H, Kracker S, Durandy A, Nonoyama S, Morio T, Imai K	16th Biennial Meeting of the European Society of Immunodeficiencies	2014年10月29日-11月1日	国外
Mutations in Bruton's tyrosine kinase impairiga responses	Mitsuiki N, Yang X, Bartol S, Kosaka Y, Takada H, Imai K, Kanegane H, Mizutani S, Van der Burg M, Van Zelm M, Ohara O, Morio T	16th Biennial Meeting of the European Society of Immunodeficiencies	2014年10月29日-11月1日	国外
B-precursor acute lymphoblastic leukemia in a patient with X-linked agammaglobulinemia	Hoshino A, Okuno Y, Migita M, Ban H, Yang X, Kiyokawa N, Kojima S, Ohara O, Kanegane H	16th Biennial Meeting of the European Society of Immunodeficiencies	2014年10月29日-11月1日	国外
Whole exome sequencing reveals atypical phenotype of X-linked lymphoproliferative syndrome.	Kanegane H	A symposium for researchers and clinicians on XLP and WAS	2014年11月3-4日	国外
Identification of myosin heavy chain 9 (MYH9) disorders in children with macrothrombocytopenia: a result from two institutions in Thailand（口頭）	Sirachainan N, Komwilaisak P, Kitamura K, Hongeng S, Sekine T, Kunishima S	Hanoi(8th Congress of the Asian-Pacific Society of Thrombosis and Hemostasis)	2014年10月	国外
Differential diagnosis of congenital macrothrombocytopenia（口頭）	Kunishima S	Hanoi(8th Congress of the Asian-Pacific Society of Thrombosis and Hemostasis)	2014年10月	国外
Whole-exome sequence analysis of Ataxia-Telangiectasia like phenotype	Masatoshi Takagi, Setsuko Hasegawa, Shuki Mizutani	12th Ataxia Telangiectasia Clinical Research Conference 2014	2014年11月15日	国外
The clinical and genetic features of dyskeratosis congenita, cryptic dyskeratosis congenita, and Hoyeraal-Hreidarsson syndrome in Japan.ポスター	Hiroki Yamaguchi, Hirotoshi Sakaguchi, Kenichi Yoshida, Miharu Yabe, Hiromasa Yabe, Yusuke Okuno, Hideki Muramatsu, Shunsuke Yui, Koiti Inokuchi, Etsuro Ito, Seishi Ogawa, Seiji Kojima.	The 56th Annual Meeting American Society of Hematology	2014年12月5-9日	国外
αIIb(R990W), a constitutive activating mutation of integrin αIIbβ3, knock-in mice show macrothrombocytopenia with impairment of platelet function（ポスター）	Kiyomizu K, Kashiwagi H, Kunishima S, Banno F, Kato H, Morikawa Y, Tadokoro S, Kokame K, Honda S, Miyata T, Kanakura Y, Tomiyama Y	The 56th Annual Meeting American Society of Hematology	2014年12月5-9日	国外
Elevated Red Cell Reduced Glutathione Is a Novel Biomarker of Diamond-Blackfan Anemia	Utsugisawa T, Uchiyama T, Ogura H, Aoki T, Shito M, Ohara A, Ishiguro A, Kojima S, Ohga S, Ito E, Kanno H	The 56th Annual Meeting American Society of Hematology	2014年12月5-9日	国外
Hematopoietic Stem Cell Transplantation for Patients with Refractory Cytopenia of Childhood（ポスター）	Hasegawa D, Hirabayashi S, Ishida Y, Watanabe S, Zaike Y, Tsuchida M, Masunaga A, Yoshimi A, Hama A, Kojima S, Ito M, Nakahara T, Manabe A,	The 56th Annual Meeting American Society of Hematology	2014年12月5-9日	国外
Central Morphology Review of Childhood Bone Marrow Failure in Japan	濱麻人、真部淳、長谷川大輔、野沢一江、奥野友介、村松秀城、高橋義行、渡邉健一郎、小原明、伊藤雅文、小島勢二	The 56th Annual Meeting American Society of Hematology	2014年12月5-9日	国外
Exploring potential usefulness of 5-aminolevulinic acid for X-linked sideroblastic anemia.(口頭)	藤原　亨、岡本　浩二、新國　僚祐、高橋　究、沖津庸子、福原　規子、大西　康、石澤　賢一、一迫玲、中村　幸夫、中島　元夫、田中　徹、張替　秀郎	The 56th Annual Meeting American Society of Hematology	2014年12月5-9日	国外
Impact of TET2 deficiency on iron metabolism in erythropoiesis: a potential link to ring sideroblast formation.（口頭）	猪倉　恭子、藤原　亨、沖津　庸子、福原　規子、大西　康、石澤　賢一、下田　克哉、張替　秀郎	The 56th Annual Meeting American Society of Hematology	2014年12月5-9日	国外
神経症状と免疫不全を呈した9症例に対する全エクソン解析	金子節子，高木正稔，今井耕輔，森尾友宏，水谷修紀	第117回日本小児科学会学術集会	2014年4月11-13日	国内

発表した成果（発表題目、口頭・ポスター発表の別）	発表者氏名	発表した場所（学会等名）	発表した時期	国内・外の別
JMMLとRALDの診断基準を同時に満たした1歳女児例	三上真充，塩田光隆，田中邦昭，壹岐陽一，本田吉孝，森嶋達也，村松秀城，井澤和司，高木正稔，秦大資	第117回日本小児科学会学術集会	2014年4月11-13日	国内
NRAS体細胞モザイク変異による自己免疫性リンパ増殖症候群様疾患の1例	楊 曦，高木正稔，菊地雅子，横田俊平，小池健一，村松秀城，小島勢二，金兼弘和	第117回日本小児科学会学術集会	2014年4月11-13日	国内
教育講演「原発性免疫不全症に合併する自己炎症」	金兼弘和	第117回日本小児科学会学術集会	2014年4月11-13日	国内
教育セミナー「原発性免疫不全症に対する皮下注用免疫グロブリンIgPro20(Hizentra®)の有効性と安全性について」	金兼弘和	第117回日本小児科学会学術集会	2014年4月11-13日	国内
NRAS体細胞モザイク変異による自己免疫性リンパ増殖症候群様疾患の１例	楊　曦，高木正稔，菊池雅子，横田俊平，小池健一，村松秀城，小島勢二，金兼弘和	第117回日本小児科学会学術集会	2014年4月11-13日	国内
わが国のFanconi貧血患者における免疫学的検討	本間健一，満生紀子，釜江智佳子，今井耕輔，森尾友宏，金兼弘和，矢部みはる，村松秀城，小島勢二，野々山恵章	第117回日本小児科学会学術集会	2014年4月11-13日	国内
XIAP欠損症における血清IL-18の持続高値	和田泰三，金兼弘和，太田和秀，谷内江昭宏	第117回日本小児科学会学術集会	2014年4月11-13日	国内
女児例を含むXIAP欠損症の同胞例	國津智彬，池田勇八，多賀　崇，野村明孝，竹内義博，松井　潤，吉田　忍，八角高裕，楊　曦，金兼弘和	第117回日本小児科学会学術集会	2014年4月11-13日	国内
芽球割合の低いTAMにおける臨床像の解析(口演)	朴 明子，外松 学，新井 心，大木 健太郎，小林 富男，丸山 憲一，鮫島 希代子，林 泰秀	第117回日本小児科学会学術集会	2014年4月11-13日	国内
Whole exome sequenceにより本邦初の*RTEL1*変異を同定したHoyeraal-Hreidarsson症候群	石村匡崇、土居岳彦、高田英俊、瀧本智仁、山元裕之、吉田健一、小川誠司、小島勢二、大賀正一、原寿郎	第117回日本小児科学会学術集会	2014年4月11-13日	国内
Molecular mechanisms for congenital macrothrombocytopenia（口頭）	國島伸治	第36回日本血栓止血学会学術集会（大阪）	2014年5月	国内
巨核球特異的β1-tubulin異常は微小管構成阻害により胞体突起形成不全を来す（口頭）	國島伸治　北村勝誠　西村智　鈴木英紀　今泉益栄　齋藤英彦	第36回日本血栓止血学会学術集会（大阪）	2014年5月	国内
α-Storage Pool病の1例（ポスター）	兼松　毅　岸本磨由子　鈴木伸明　國島伸治　松下正	第36回日本血栓止血学会学術集会（大阪）	2014年5月	国内
CD40LG and SIL1 mutations associated with neurodegeneration and hypogammaglobulinemia	Hasegawa S, Takagi M, Sunagawa Y, Imai K, Morio T, Mizutani S	第56回日本小児神経学会学術集会	2014年5月29日	国内
新生児・乳児期に発症する先天性溶血性貧血の病因と診断	菅野　仁	第24回日本産婦人科新生児血液学会（横浜）	2014年6月13-14日	国内
Diamond-Blackfan貧血の病態診断（ワークショップ	伊藤悦朗	第24回日本産婦人科新生児血液学会（横浜）	2014年6月13-14日	国内
MYH9異常症の体細胞モザイク（口頭）	國島伸治　北村勝誠　松本多絵　関根孝司	第15回日本検査血液学会学術集会（仙台）	2014年7月	国内
小児における血液疾患の診断.	小島勢二	第15回日本検査血液学会学術集会（仙台）	2014年7月20日	国内
ファンコニ貧血症とDNA修復メカニズム（招待講演）	髙田　穣	第３６回日本光医学・光生物学会シンポジウム　大阪大学銀杏会館	2014年7月25日	国内
DBAにおける貧血と身体徴候の浸透率に関して	大賀正一、菅野仁、伊藤悦朗、小島勢二	「稀少小児遺伝性血液疾患に対する新規責任遺伝子の探索と遺伝子診断システムの構築に関する研究」　小島班 「小児およびAYA世代の増殖性血液疾患の診断精度向上と診療ガイドラインの改訂のための研究」　林班 「先天性骨髄不全症の登録システムの構築と診断ガイドラインの作成に関する研究」　伊藤班 3班合同班会議	2014年8月1日	国内
幹細胞技術の検査医学研究への応用（口頭）	國島伸治	名古屋（第33回日本臨床検査医学会東海北陸支部例会）	2014年8月	国内
原因不明のIgA欠損症としてフォローされていたactivated P13K-δ syndromeの一例	西田直徳，星野顕宏，足立雄一，金兼弘和，渡辺祐紀，中林玄一，荒木来太，西村良成，和田泰三，谷内江昭宏	第46回小児科感染症学会	2014年8月18-19日	国内
遺伝性DNA修復異常疾患：家族性乳がんとファンコニ貧血（招待講演）	髙田　穣	日本家族性腫瘍学会 第１７回家族性腫瘍セミナー 近畿大学・東大阪キャンパス	2014年8月24日	国内
眼球運動失行と低アルブミン血症を伴う早期発症型失調症9例の免疫学的検討	加藤環，今井耕輔，高木正稔，横関明男，小野寺理，野々山恵章	第5回関東甲信越免疫不全症研究会	2014年9月21日	国内

発表した成果（発表題目、口頭・ポスター発表の別）	発表者氏名	発表した場所（学会等名）	発表した時期	国内・外の別
多様自己抗体陽性の免疫調節異常症1乳児例	緒方昌平，竹内恵美子，野元けいこ，扇原義人，江波戸孝輔，紺野寿，坂東由紀，高木正稔，石井正浩	第5回関東甲信越免疫不全症研究会	2014年9月21日	国内
Whole exome sequenceにより本邦初の*RTEL1*変異を同定したHoyeraal-Hreidarsson症候群	石村 匡崇、土居 岳彦、 高田 英俊、 瀧本 智仁、山元 裕之、白石 暁、吉田 健一、小川 誠司、小島勢二、大賀 正一、原 寿郎	第42回日本臨床免疫学会総会	2014年9月25-27日	国内
早老症Hutchinson-Gilford症候群の全国疫学調査：診療ガイドライン策定に向けて	井原健二、原 寿郎、大賀正一、竹本 稔、横手幸太郎	第48回日本小児内分泌学会	2014年9月25-27日	国内
相同組換え修復の細胞周期依存性解析	坂本 裕貴，大川 沙織，穀田 哲也，勅使河原 愛，飯島 健太，高田 穣，小松 賢志，田内 広	日本放射線影響学会第５７回大会　鹿児島市	2014年10月1-3日	国内
DNA鎖間架橋除去におけるFAN1ヌクレアーゼの役割	高橋 大介，佐藤 浩一，平山 恵美子，高田 穣，胡桃坂 仁志	第87回日本生化学会大会　京都市	2014年10月15-18日	国内
Comprehensive analysis of Japanese Fanconi anemia (FA) patients has led to the identification of an E2 enzyme UBE2T as a novel FA gene.	Minoru Takata	第５回日米修復会議エクシブ鳴門	2014年10月29日	国内
GT-like phenotype with macrothrombocytopenia induced by αIIbβ3 activating mutation in mice（口頭）	Kiyomizu K, Kashiwagi H, Kunishima S, Banno F, Kato H, Morikawa Y, Tadokoro S, Kokame K, Honda S, Miyata T, Kanakura Y, Tomiyama Y	第76回日本血液学会学術集会（大阪）	2014年10月31日-11月2日	国内
疾患特異的iPS細胞を用いた先天性好中球減少症の病態解析	渡邉健一郎	第76回日本血液学会学術集会（大阪）	2014年10月31日-11月2日	国内
ダウン症候群の造血異常（教育講演）	伊藤悦朗	第76回日本血液学会学術集会（大阪）	2014年10月31日-11月2日	国内
Insight into molecular mechanisms of pathology in Diamond-Blackfan Anemia（シンポジウム：Recent advance in genetic abnormalities of hereditary hematologic disorders）	土岐　力，伊藤悦朗	第76回日本血液学会学術集会（大阪）	2014年10月31日-11月2日	国内
ALDH2 polymorphism in patients with Diamond-Blackfan anemia in Japan	池田史圭	第76回日本血液学会学術集会（大阪）	2014年10月31日-11月2日	国内
口頭 Exploring the potential usefulness of 5-aminolevulinic acid (ALA) for sideroblastic anemia.	新國　僚祐、藤原　亨、沖津　庸子、福原　規子、大西　康、石澤　賢一、一迫　玲、田中　徹、張替　秀郎	第76回日本血液学会学術集会（大阪）	2014年10月31日-11月2日	国内
CSF3R and CALR mutations and cytogenetic findings in pediatric myeloid malignancies(口演)	Sano H, Ohki K, Park M, Shiba N, Hara Y, Sotomatsu M, Tomizawa D, Taga T, Kiyokawa N, Tawa A, Horibe K, Adachi A, Hayashi Y	第76回日本血液学会学術集会（大阪）	2014年10月31日-11月2日	国内
Diamond-Blackfan 貧血（DBA）母子の診断における全エクソーム解析の有用性	市村卓也、湯尻俊昭、下村麻衣子、永井功造、西眞篤、吉田健一、小川誠司、奥野友介、村松秀城、小島勢二、菅野仁、伊藤悦朗、大賀正一	第76回日本血液学会学術集会（大阪）	2014年10月31日-11月2日	国内
原因不明先天性溶血性貧血症例の全エクソーム解析による膜骨格蛋白遺伝子変異の同定	市東正幸、青木貴子、槍澤大樹、小倉浩美、大賀正一、岩井朝幸、末延聡一、伊藤悦朗、奥野裕介、小島勢二、小川誠司、菅野仁	第76回日本血液学会学術集会（大阪）	2014年10月31日-11月2日	国内
Long-term outcome of 100 children with moderate aplastic anemia	Yagasaki H, Yabe H, Ohara A, Kosaka Y, Kudo K, Kobayashi R, Ohga S, Morimoto A, Watanabe K, Muramatsu H, Takahashi Y, Kojima S.	第76回日本血液学会学術集会（大阪）	2014年10月31日-11月2日	国内
JAK2, *MPL*, and *CALR* mutations in children with essential thrombocythemia	Sekiya Y, Okuno Y, Muramatsu H, Olfat I, Kawashima N, Narita A, Wang X, Xu Y, Hama A, Fujisaki H, Toshihiko I, Hasegawa D, Kosaka Y, Sunami S, Ohtsuka Y, Ohga S, Takahashi Y, Kojima S, Shimada A.	第76回日本血液学会学術集会（大阪）	2014年10月31日-11月2日	国内
原因不明先天性溶血性貧血症例の全エクソーム解析による膜骨格蛋白遺伝子変異の同定	市東　正幸、青木貴子、槍澤大樹、小倉浩美、大賀正一、岩井朝幸、末延聡一、伊藤悦朗、奥野友介、小島勢二、小川誠司、菅野 仁	第76回日本血液学会学術集会（大阪）	2014年10月31日-11月2日	国内
我が国におけるG6PD異常症の現状	菅野　仁、青木貴子、市東正幸、槍澤大樹、小倉浩美	第76回日本血液学会学術集会（大阪）	2014年10月31日-11月2日	国内
小児再生不良性貧血の治療	小島勢二	第76回日本血液学会学術集会（大阪）	2014年10月31日-11月2日	国内
病因未確定の先天性溶血性貧血に対する全エクソーム解析	青木貴子、市東正幸、小倉浩美、高橋秀弘、岩井朝幸、濱端隆行、渡邉健一郎、常松健一郎、奥野友介、村松秀城、吉田健一、宮野悟、大賀正一、小川誠司、小島勢二、菅野 仁	日本人類遺伝学会第59回大会（東京）	2014年11月	国内
UBE2T is a novel FA gene identified in Japanese Fanconi anemia patients	Minoru Takata, Asuka Hira, Kenichi Yoshida, Koichi Sato, Akira Shimamoto, Hidetoshi Tahara, Hitoshi Kurumizaka, Seishi Ogawa, Hiromasa Yabe, and Miharu Yabe	The 9th 3R Symposium Gotemba Kogen Hotel	2014年11月17-21日	国内
Identification of novel UBE2T mutations in Japanese Fanconi anemia patients　口演	Hira A, Yoshida K, Sato K, Shimamoto A, Tahara H, Kurumizawa H, Ogawa S, Takata M, Yabe H, Yabe M	第37回日本分子生物学会年会　横浜市	2014年11月25-27日	国内
日本人ファンコニ貧血患者における新規原因遺伝子UBE2Tの同定	平 明日香，吉田 健一，佐藤 浩一，嶋本 顕，田原 栄俊，胡桃坂 仁志，小川 誠司，高田 穣，矢部 普正，矢部 みはる	第37回日本分子生物学会年会　横浜市	2014年11月25-27日	国内
ファンコニ貧血経路とそのキータンパク質FANCD2の機能解析	高田 穣，勝木 陽子，佐藤 浩一，石合 正道，胡桃坂 仁志	第37回日本分子生物学会年会　横浜市	2014年11月25-27日	国内

発表した成果（発表題目、口頭・ポスター発表の別）	発表者氏名	発表した場所（学会等名）	発表した時期	国内・外の別
ゲノム編集酵素によるファンコニ貧血原因遺伝子FANCAのノックアウト細胞作製の試み	久野 真央，平 明日香，高田 穣	第37回日本分子生物学会年会　横浜市	2014年11月25-27日	国内
日本人ファンコニ貧血患者における新規原因遺伝子UBE2Tの同定	平 明日香，吉田 健一，佐藤 浩一，嶋本 顕，田原 栄俊，胡桃坂 仁志 小川 誠司，高田 穣，矢部 普正，矢部 みはる	第37回日本分子生物学会年会　横浜市	2014年11月25-27日	国内
ファンコニ貧血経路とそのキータンパク質FANCD2の機能解析	高田 穣，勝木 陽子，佐藤 浩一，石合 正道，胡桃坂 仁志	第37回日本分子生物学会年会　横浜市	2014年11月25-27日	国内
Fanconi貧血患者にみられるFANCD2変異体の機能解析	佐藤 浩一，石合 正道，高田 穣，胡桃坂 仁志	第37回日本分子生物学会年会　横浜市	2014年11月25-27日	国内
DNA鎖間架橋修復で働くFAN1ヌクレアーゼの生化学的機能解析	平山 恵美子，高橋 大介，佐藤 浩一，高田 穣，胡桃坂 仁志	第37回日本分子生物学会年会　横浜市	2014年11月25-27日	国内
新規ACTN1変異による先天性巨大血小板性血小板減少症の1例（ポスター）	安冨素子　國島伸治　岡崎新太郎　土田晋也　鈴木孝二　吉川利英　谷澤昭彦　大嶋勇成	第56回日本小児血液・がん学会学術集会（岡山）	2014年11月28-30日	国内
発熱時の採血を契機としてMay-Hegglin異常の診断に至った男児例（ポスター）	西村美穂　伊藤早織　中川慎一郎　松尾陽子　大園秀一　上田耕一郎　稲田浩子　松石豊次郎　國島伸治	第56回日本小児血液・がん学会学術集会（岡山）	2014年11月28-30日	国内
ダウン症における一過性異常骨髄増殖症の形態学的特徴　JPLSG TAM-10形態中央診断の解析（口演）	濱 麻人，村松 秀城，長谷川 大輔，朴 明子，岩本 彰太郎，多賀 崇，伊藤 悦朗，柳沢 龍，康 勝好，林 泰秀，足立 壮一，水谷 修紀，渡邉 健一郎	第56回日本小児血液・がん学会学術集会（岡山）	2014年11月28-30日	国内
芽球割合の低いTAMにおける臨床像の解析（ポスター）	朴 明子，新井 心，大木 健太郎，外松 学，林 泰秀	第56回日本小児血液・がん学会学術集会（岡山）	2014年11月28-30日	国内
免疫不全症とリンパ増殖性疾患	金兼弘和	第56回日本小児血液・がん学会学術集会	2014年11月28-30日	国内
間質性肺野病変で発症しDermatopathic Lymphadenitisと診断された慢性肉芽腫症の男児例 Chronic granulomatous disease diagnosed as Dermatopathic lymphadenitis initially presented with diffuse pulmonary infiltration	鬼頭俊幸，山口悦郎，藤井公人，高橋恵美子，小田紘嗣，小原収，金兼弘和	第56回日本小児血液・がん学会学術集会	2014年11月28-30日	国内
Elevated red cell reduced glutathione is a novel biomarker of Diamond-Blackfan anemia	Utsugisawa T, Uchiyama T, Ogura H, Aoki T, Ohara A, Ishiguro A, Kojima S, Ohga S, Ito E, Kanno H.	San Francisco (56th ASH Annual Meeting& Exposition)	2014年12月	国外
著明なTリンパ球減少に伴いニューモシスチス肺炎を合併したランゲルハンス細胞組織球症の乳児例.　（口演）	川原勇太、和田聖哉、植田綾子、尾﨑理史、新島瞳、早瀬朋美、森本 哲.	第39回LCH研究会	2015年3月15日	国内

2．学会誌・雑誌等における論文掲載

	掲載した論文（発表題目）	発表者氏名	発表した場所（学会誌・雑誌等名）	発表した時期	国内・外の別
1	Whole-exome sequence analysis of ataxia telangiectasia-like phenotype	Hasegawa, S. Imai, K. Yoshida, K. Okuno, Y. Muramatsu, H. Shiraishi, Y. Chiba, K. Tanaka, H. Miyano, S. Kojima, S. Ogawa, S. Morio, T. Mizutani, S. Takagi, M.	Journal of the neurological sciences	2014	国外
2	Ulk1-mediated Atg5-independent macroautophagy mediates elimination of mitochondria from embryonic reticulocytes.	Honda S, Arakawa S, Nishida Y, Yamaguchi H, Ishii E, Shimizu S	Nat Commun	2014	国外
3	Long-term outcome after immunosuppressive therapy with horse or rabbit antithymocyte globulin and cyclosporine for severe aplastic anemia in children.	Jeong DC, Chung NG, Cho B, Zou Y, Ruan M, Takahashi Y, Muramatsu H, Ohara A, Kosaka Y, Yang W, Kim HK, Zhu X, Kojima S	Haematologica	2014	国外
4	Aldehyde dehydrogenase-2 polymorphism contributes to the progression of bone marrow failure in children with idiopathic aplastic anaemia.	Kawashima N, Narita A, Wang X, Xu Y, Sakaguchi H, Doisaki S, Muramatsu H, Hama A, Nakanishi K, Takahashi Y, Kojima S.	Br J Haematol	2014	国外
5	TUBB1 mutation disrupting microtubule assembly impairs proplatelet formation and results in congenital macrothrombocytopenia.	Kunishima S, Nishimura S, Suzuki H, Imaizumi M, Saito H	Eur J Haematol	2014	国外
6	GATA2 regulates differentiation of bone marrow-derived mesenchymal stem cells	Mayumi Kamata, Yoko Okitsu, Tohru Fujiwara, Masahiko Kanehira, Shinji Nakajima, Taro Takahashi, Ai Inoue, Noriko Fukuhara, Yasushi Onishi, Kenichi Ishizawa, Ritsuko Shimizu, Masayuki Yamamoto, Hideo Harigae	Haematologica	2014	国外
7	Simple diagnosis of STAT1 gain-of-function alleles in patients with chronic mucocutaneous candidiasis.	Mizoguchi Y, Tsumura M, Okada S, Hirata O, Minegishi S, Imai K, Hyakuna N, Muramatsu H, Kojima S, Ozaki Y, Imai T, Takeda S, Okazaki T, Ito T, Yasunaga S, Takihara Y, Bryant VL, Kong XF, Cypowyj S, Boisson-Dupuis S, Puel A, Casanova JL, Morio T, Kobayashi M.	Journal of Leukocyte Biology	2014	国外
8	Genetic correction of HAX1 in induced pluripotent stem cells from a patient with severe congenital neutropenia improves defective granulopoiesis.	Morishima T, Watanabe K, Niwa A, Hirai H, Saida S, Tanaka T, Kato I, Umeda K, Hiramatsu H, Saito MK, Matsubara K, Adachi S, Kobayashi M, Nakahata T, Heike T.	Haematologica	2014	国外
9	Platelet diameters in inherited thrombocytopenias: Analysis of 376 patients with all known disorders.	Noris P, Biino G, Pecci A, Civaschi E, Savoia A, Seri M, Melazzini F, Loffredo G, Russo G, Bozzi V, Notarangelo LD, Gresele P, Heller P, Pujol-Moix N, Kunishima S, Cattaneo M, Bussel J, De Candia E, Cagioni C, Ramenghi U, Cagioni C, Fabris F, Balduini CL	Blood	2014	国外
10	High serum osteopontin levels in pediatric patients with high risk Langerhans cell histiocytosis.	Oh Y, Morimoto A, Shioda Y, Imamura T, Kudo K, Imashuku S	Cytokine	2014	国外
11	Peripheral blood lymphocyte telomere length as a predictor of response to immunosuppressive therapy in childhood aplastic anemia	Sakaguchi H, Nishio N, Hama A, Kawashima N, Wang X, Narita A, Doisaki S, Xu Y, Muramatsu H, Yoshida N, Takahashi Y, Kudo K, Moritake H, Nakamura K, Kobayashi R, Ito E, Yabe H, Ohga S, Ohara A, Kojima S; Japan Childhood Aplastic Anemia Study Group	Haematologica	2014	国外
12	Impaired hematopoietic differentiation of RUNX1-mutated induced pluripotent stem cells derived from FPD/AML patients	Sakurai M, Kunimoto H, Watanabe N, Fukuchi Y, Yuasa S, Yamazaki S, Nishimura T, Sadahira K, Fukuda K, Okano H, Nakauchi H, Morita Y, Matsumura I, Kudo K, Ito E, Ebihara Y, Tsuji K, Harada Y, Harada H, Okamoto S, Nakajima H.	Leukemia	2014	国外
13	Spectrum of the mutations in Bernard-Soulier syndrome.	Savoia A, Kunishima S, De Rocco D, Zieger B, Rand ML, Pujol-Moix N, Caliskan U, Pecci A, Noris P, Srivastava A, Ward C, Kopp MC, Alessi MC, Bellucci S, Beurrier P, de Maistre E, Favier R, Hezard N, Hurtaud-Roux MF, Latger-Cannard V, Lavenu-Bombled C, Meunier S, Negrier C, Nurden A, Proulle V, Randrianaivo H, Fabris F, Platokouki H, Rosenberg H, Gargouri AF, Heller P, Karimi M, Balduini CL, Pastore A, Lanza F	Hum Mut	2014	国外
14	Pulmonary fibrosis associated with TINF2 gene mutation: is somatic reversion required?	Tanino Y, Yamaguchi H, Fukuhara A, Munakata M.	Eur Respir J.	2014	国外

	掲載した論文（発表題目）	発表者氏名	発表した場所（学会誌・雑誌等名）	発表した時期	国内・外の別
15	Effect of 5-aminolevulinic acid on erythropoiesis: a preclinical in vitro characterization for the treatment of congenital sideroblastic anemia.	Tohru Fujiwara, Koji Okamoto, Ryouyu Niikuni, Kiwamu Takahashi, Yoko, Okitsu, Noriko Fukuhara, Yasushi Onishi, Kenichi Ishizawa, Ryo Ichinohasama, Yukio Nakamura, Motowo Nakajima, Tohru Tanaka, Hideo Harigae	Biochem Biophys Res Commun	2014	国外
16	Mutations in Kruppel-like factor 1 cause transfusion-dependent hemolytic anemia and persistence of embryonic globin gene expression.	Viprakasit V, Ekwattanakit S, Riolueang S, Chalaow N, Fisher C, Lower K, Kanno H, Tachavanich K, Bejrachandra S, Saipin J, Juntharaniyom M, Sanpakit K, Tanphaichitr VS, Songdej D, Babbs C, Gibbons RJ, Philipsen S, Higgs DR.	Blood	2014	国外
17	First-line treatment for severe aplastic anemia in children: bone marrow transplantation from a matched family donor vs. immunosuppressive therapy	Yoshida N, Kobayashi R, Yabe H, Kosaka Y, Yagasaki H, Watanabe KI, Kudo K, Morimoto A, Ohga S, Muramatsu H, Takahashi Y, Kato K, Suzuki R, Ohara A, Kojima S	Haematologica	2014	国外
18	Recurrent CDC25C mutations drive malignant transformation in FPD/AML	Yoshimi A, Toya T, Kawazu M, Ueno T, Tsukamoto A, Iizuka H, Nakagawa M, Nannya Y, Arai S, Harada H, Usuki K, Hayashi Y, Ito E, Kirito K, Nakajima H, Ichikawa M, Mano H, Kurokawa M.	Nat Commun.	2014	国外
19	ACTN1-related thrombocytopenia: identification of novel families for phenotypic characterization.	Bottega R, Marconi C, Faleschini M, Baj G, Cagioni C, Pecci A, Pippucci T, Ramenghi, U, Pardini S, Ngu L, Baronci C, Kunishima S, Balduini CL, Seri M, Savoia A, Noris P	Blood	2015	国外
20	Criteria for evaluating response and outcome in clinical trials for children with juvenile myelomonocytic leukemia.	Niemeyer CM, Loh ML, Cseh A, Cooper T, Dvorak CC, Chan R, Xicoy B, Germing U, Kojima S, Manabe A, Dworzak M, Demoerloose B, Stary J, Smith OP, Masetti R, Catala A, Berqstraesser E, Ussowicz M, Fabri O, Baruchel A, Cace H, Zwaan M, Locatelli F, Hasle H, van den Heuvel-Eibrink MM, Flotho C, Yoshimi A.	Haematologica	2015	国外

Ⅳ．研究成果の刊行物・別刷り

Journal of the Neurological Sciences 340 (2014) 86–90

Contents lists available at ScienceDirect

Journal of the Neurological Sciences

journal homepage: www.elsevier.com/locate/jns

Whole-exome sequence analysis of ataxia telangiectasia-like phenotype

Setsuko Hasegawa [a], Kohsuke Imai [a], Kenichi Yoshida [b,e], Yusuke Okuno [b], Hideki Muramatsu [c], Yuichi Shiraishi [f], Kenichi Chiba [f], Hiroko Tanaka [d], Satoru Miyano [d], Seiji Kojima [c], Seishi Ogawa [b,e], Tomohiro Morio [a], Shuki Mizutani [a], Masatoshi Takagi [a,*]

[a] Department of Pediatrics and Developmental Biology, Tokyo Medical and Dental University, Tokyo, Japan
[b] Cancer Genomics Project, Graduate School of Medicine, University of Tokyo, Tokyo, Japan
[c] Department of Pediatrics, Nagoya University Graduate School of Medicine, Nagoya, Japan
[d] Laboratory of Sequence Analysis, Human Genome Center, Institute of Medical Science, The University of Tokyo, Tokyo, Japan
[e] Department of Pathology and Tumor Biology, Graduate School of Medicine, Kyoto University, Kyoto, Japan
[f] Laboratory of DNA Information Analysis, Human Genome Center, Institute of Medical Science, The University of Tokyo, Tokyo, Japan

ARTICLE INFO

Article history:
Received 2 December 2013
Received in revised form 21 February 2014
Accepted 25 February 2014
Available online 4 March 2014

Keywords:
Whole-exome sequencing
Neurodegeneration
Immunodeficiency
CD40 ligand
SIL1
DNA damage

ABSTRACT

A number of diseases exhibit neurodegeneration with/without additional symptoms such as immunodeficiency, increased cancer risk, and microcephalus. Ataxia telangiectasia and Nijmegen breakage syndrome, for example, develop as a result of mutations in genes involved in the DNA damage response. However, such diseases can be difficult to diagnose as they are only rarely encountered by physicians. To overcome this challenge, nine patients with symptoms that resemble those of ataxia telangiectasia, including neurodegeneration, hypogammaglobulinemia, telangiectasia, and/or elevated serum α-fetoprotein, were subjected to whole-exome sequencing (WES) to identify the causative mutations. Molecular diagnosis was achieved in two patients: one displayed CD40 ligand (CD40LG) deficiency, while a second showed a homozygous *SIL1* mutation, which has been linked to Marinesco-Sjögren syndrome (MSS). Typical features of CD40LG deficiency and MSS are distinct from the symptoms usually seen in ataxia telangiectasia. These dissociations between phenotype and genotype make it difficult to achieve molecular diagnosis of orphan diseases. Whole-exome sequencing analyses will assist in the molecular diagnosis of such cases and allow the identification of genotypes that would not be expected from the phenotype.

1. Introduction

Neurodegenerative disease is characterized by progressive nervous system dysfunction. Primary immunodeficiency is a disorder of immune regulation. Occasionally, progressive nervous system dysfunction and primary immunodeficiency can occur together within single disorders, and the genes responsible for such conditions have been identified. Ataxia telangiectasia (A-T) is one such disorder involving progressive cerebellar ataxia and immunodeficiency, as well as conjunctival telangiectasia. The gene responsible, *ATM*, plays a central role in the DNA damage response (DDR) [1]. Mutations of *NBS1* and *Mre11*, genes also involved in DDR network, can give rise to phenotypically A-T-like patients, such as those with Nijmegen breakage syndrome (NBS) and A-T-like disease (ATLD). Not only NBS and ATLD, but also a number of diseases also feature both neurological symptoms and immunodeficiency. Gatti et al. proposed a disease category named XCIND (X-ray irradiation sensitivity, Cancer susceptibility, Immunodeficiency, Neurological abnormality, Double strand DNA breakage) syndrome [2], in which failure of the DDR pathway results in genome instability and an increased risk of cancer. A number of human genetic disorders are characterized by a defective DDR pathway and feature neurodegeneration, which suggests that maintaining genome stability is also important for preserving post-mitotic neurons [3].

Pediatric neurodevelopmental disorders comprise various diseases with multi-system symptoms. Some of the features characteristic of these diseases appear only in later years, and some patients only manifest non-specific symptoms, leading to a delayed diagnosis. In certain cases, different phenotypes can arise from the same genotype. For example, mutation of SETX, which is involved in DDR, can give rise to three distinct types of disease: ataxia-ocular apraxia-2 (AOA2), autosomal recessive spinocerebellar ataxia (SCA) 1, and juvenile amyotrophic lateral sclerosis (ALS) 4. In the present study, nine patients with clinical features of neurodegeneration, hypogammaglobulinemia and/or telangiectasia were analyzed by whole-exome sequencing (WES). The

* Corresponding author at: Department of Pediatrics and Developmental Biology, Graduate Medical School, Tokyo Medical and Dental University, Yushima 1-5-45, Bunkyo-ku, Tokyo 113-8519, Japan. Tel.: +81 3 5803 5249; fax: +81 3 5803 5247.
E-mail address: m.takagi.ped@tmd.ac.jp (M. Takagi).

http://dx.doi.org/10.1016/j.jns.2014.02.033
0022-510X/

results reveal that one patient had CD40LG deficiency and that another patient had Marinesco–Sjögren syndrome (MSS).

2. Materials and methods

2.1. Patient samples

Patients with neurological symptoms resembling an A-T-like phenotype, comprised mainly of cerebellar ataxia plus hypogammaglobulinemia, telangiectasia and/or elevated serum alpha-fetoprotein (AFP), were recruited. ATM western blotting was performed with these patients to exclude A-T. Patients with normal ATM levels were subjected to WES.

Patients provided informed written consent, and the experimental design was approved by the ethics committee at Tokyo Medical and Dental University (No. 103).

2.2. Whole-exome sequencing analysis (WES)

WES analysis was performed as previously described [4]. Briefly, genomic DNA was fragmented, and exonic sequences were enriched using SureSelect Target Enrichment with the SureSelect Human All Exon 38 Mb kit (Agilent). The captured fragments were purified and sequenced on an Illumina Hiseq2000 platform using paired-end reads. Bioinformatic analysis was performed using an in-house algorithm based on published tools. Identified single nucleotide variants (SNVs) were filtered using dbSNP version 131 and 132, the 1000 Genomes database, an in-house SNP database, and the Human Genetic Variation Database (HGVD) (http://www.genome.med.kyoto-u.ac.jp/SnpDB/).

2.3. Genome sequencing

The mutations identified by WES were confirmed by direct sequencing. Genomic DNA from peripheral blood mononuclear cells was obtained using the QIAamp DNA Mini kit (Qiagen). Exons of the respective genes were amplified by PCR. Nucleotide sequencing was performed by cycle sequencing using ABI BigDye Terminator chemistry (Applied Biosystems) followed by capillary electrophoresis on an ABI 3100 automated sequencer.

2.4. CD40LG expression analysis

CD40LG expression was measured by flow cytometry using activated T-cells [5]. Cells were treated with phosphate-buffered saline (PBS) or PMA/ionomycin, and incubated for 4 h. CD40LG expression in T-cell gates was monitored by phycoerythrin (PE)-conjugated anti-human CD40LG antibody (Beckman Coulter), combined with the T-cell marker CD3 (PC 5-conjugated anti-CD3 antibody: Beckman Coulter). Flow cytometric analysis was performed using FACS Caliber with the CellQuest program (Becton-Dickinson).

2.5. Western blotting

Cells were lysed in RIPA buffer (50 mM Tris–HCl (pH 7.5), 150 mM NaCl, 0.5% sodium deoxycholate, 0.1% SDS, phosphatase, and a protease inhibitor cocktail). Samples were resolved on SDS-polyacrylamide gels. The gels were transferred to nitrocellulose membranes (Millipore) and blocked with 5% nonfat milk. The membranes were incubated with the appropriate anti-SIL1 (Abcam), anti-β-actin (Sigma), anti-eIF2α, and anti-phospho-eIF2α (Cell Signaling) antibodies. Primary antibodies were detected by binding horseradish peroxidase (HRP)-conjugated anti-rabbit or anti-mouse secondary antibody with an ECL kit (GE Healthcare).

3. Results

Patients presenting with more than two features of ataxia or other neurological degeneration symptoms and hypogammaglobulinemia, telangiectasia and/or elevated serum AFP were examined in this study (Table 1). Most of the causative ATM mutations in typical A-T patients are truncating, and ATM protein is therefore absent in these patients [6]. Western blot analysis confirmed ATM protein expression in all of the subjects in this study (data not shown). Furthermore, WES analysis failed to identify an ATM mutation, and thus A-T was ruled out in these subjects. We speculated that these patients had XCIND syndrome. WES revealed 238 non-synonymous SNV, frameshift, or splice site mutations. Although SNVs located within DDR-related genes were identified (Supplementary Table 1), no mutations were seen in the genes responsible for XCIND (data not shown). Intriguingly, a hemizygous *CD40LG* mutation and a homozygous *SIL1* mutation were identified in patients 1 and 5, respectively.

3.1. Patient 1

Patient 1 is a 21-year-old male and a child of non-consanguineous healthy Japanese parents. He has no familial history of any immunological disorders, while his grandfather suffered from Parkinson's disease. He showed normal motor development during infancy, but failed to thrive. Due to recurrent otitis media, he was presumed to have a primary immune deficiency of unknown origin, and began intravenous immunoglobulin treatment every 2 weeks at 12 months of age. In childhood, he manifested clumsiness, and an asymmetrical arm motion was identified during walking at 16 years of age. At 20 years, he developed involuntary movements that were induced by eating and that deteriorated over a few days. He was admitted with involuntary movements of the extremities; he was alert and conscious. His intelligence quotient was 58. He had mild dysarthria. Neurologic examinations

Table 1
Clinical features of patients.

patient	Sex	Age (years)	Immunodeficiency	Neurological symptoms	Telangiectasia	Serum AFP
1	M	21	Recurrent otitis media, low IgG, and elevated IgM	Choreoathetosis, dysarthria, hyperreflexia, psychomotor retardation, and cerebral cortex atrophy	−	NE
2	F	5	–	Ataxia and cerebellar atrophy	+	Normal
3	F	21	Low IgA and normal IgG and IgM	Nystagmus, dysarthria, hypotonus, myoclonus, ataxia, hyporeflexia, and cerebellar atrophy	+	Normal
4	F	2	Low IgG	Psychomotor retardation and regression	−	Elevated
5	M	1	Low IgG and IgG_2 subclass and normal IgM	Gross motor developmental delay, nystagmus, and cerebellar atrophy	−	Normal
6	F	1	–	Myoclonus, choreoathetosis, psychomotor retardation, and epilepsy	−	Elevated
7	F	11	Aspergillosis and low IgA, IgG and IgM	Psychomotor retardation and epilepsy	−	Normal
8	F	7	Oral candidiasis, *Pneumocystis carinii* pneumonia, and low IgA, IgG and IgM	Psychomotor retardation	−	NE
9	F	5	Low IgM and reduced B cell number	Ataxia, mental retardation, and microcephaly	+	NE

NE: not examined.

showed involuntary movements of the limbs, face, and trunk. This non-rhythmic involuntary movement appeared dominant in the right arm, and was induced by motor action. This movement did not occur during sleep. The deep tendon reflex was markedly hyperactive in the bilateral ankle clonus, but there was no pathological reflex.

Laboratory data showed normal complete blood cell count with no acanthocytes. Electrolyte and hepato-renal functions were within normal limits, and euthyroidism was confirmed. Serological examination showed low serum levels of IgG (687 mg/dl) and elevated serum IgM (462 mg/dl). Serum ceruloplasmin levels were normal, and the autoantibodies, anti-streptolysin O and anti-streptokinase antibodies, were negative. The cerebrospinal fluid cell count was 21 cells/mm^3 and comprised 100% mononuclear cells. Protein and glucose concentrations were 21 mg/dl and 54 mg/dl, respectively. No pathogens indicating infection were identified. There was no calcification at the time of brain computed tomography (CT). Brain magnetic resonance imaging (MRI) revealed cerebral cortex atrophy without abnormal signal intensity and atrophy of the striatum (Fig. 1). Electroencephalography demonstrated generalized intermittent slow waves and focal sharp waves over the bilateral occipital region. He had no clinical seizures. Within 6 months, he was unable to walk or sit unaided, as a consequence of choreoathetosis.

WES identified a *CD40LG* mutation in this patient, which was validated by Sanger sequencing (Fig. 2A). A functional assay for CD40LG expression confirmed that the mutation impaired CD40LG functioning (Fig. 2B).

3.2. Patient 5

Patient 5 is a 14-month-old male and a child of non-consanguineous healthy Japanese parents. He has no familial history of any immunological disorder. His sister (6 years old) and brother (3 years old) have had several febrile seizures. He was born uneventfully, and showed mild developmental delay. He was able to hold his head up at 10 months of age, rolled over at 12 months, and has yet to sit up and crawl. He showed nystagmus at 12 months and his brain MRI revealed cerebellar atrophy (Fig. 3). Serological examination showed relatively low serum levels of IgG (490 mg/dl), IgG$_2$ subclass (18%), and IgA (15 mg/dl) and normal serum levels of IgM (68 mg/dl). Opportunistic infections or recurrent

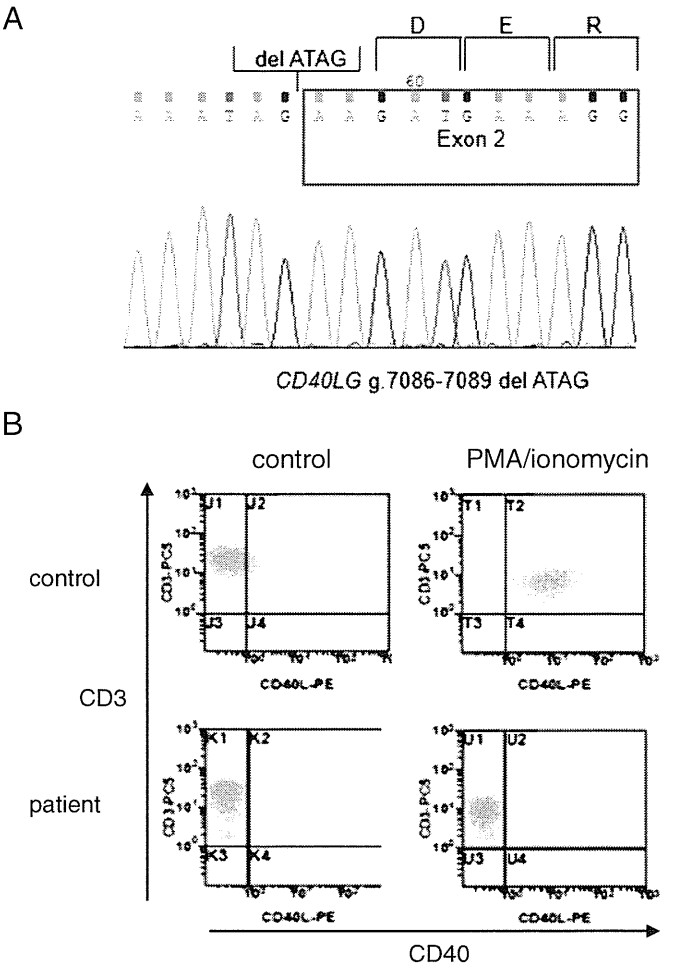

Fig. 2. A, Sequence electropherogram of *CD40LG*. A hemizygous frameshift mutation was identified. B, PMA/ionomycin treatment induced CD40LG expression. 88.68% of CD3$^+$CD8$^-$ cells were positive for CD40LG in healthy controls. On the other hand, only 0.82% were positive in patient-derived activated T-cells.

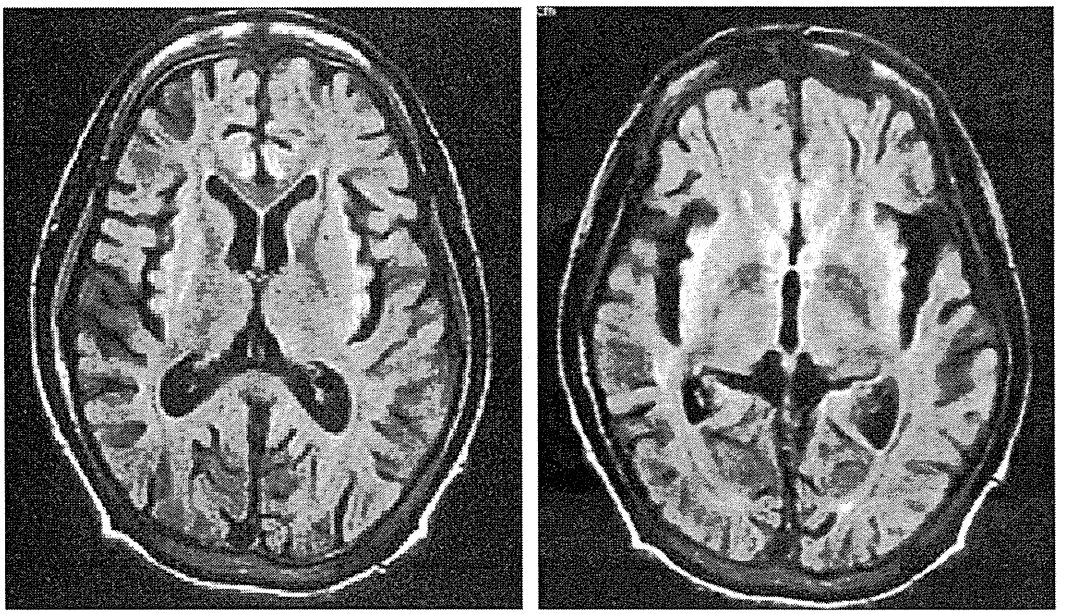

Fig. 1. Fluid attenuated inversion recovery axial images of patient 1, demonstrating cerebral cortical atrophy.

infections have not been observed in this patient. Cerebrospinal fluid analysis was normal, as were levels of pyruvate and lactate.

Although hypoglobulinemia has not been previously reported in MSS, WES identified a homozygous frameshift mutation in *SIL1*, c.936_937ins G, which was validated by Sanger sequencing (Fig. 4A). SIL1 expression was markedly decreased in a patient-derived EB virus-transformed lymphoblastoid cell line (Fig. 4B). SIL1 functions in combination with binding immunoglobulin protein (BiP) to ensure proper folding of proteins in the endoplasmic reticulum (ER) [7]. Accumulation of misfolded proteins suppresses de novo protein synthesis via translation inhibition. eIF2α is involved in this process. ER stress induces phosphorylation of eIF2α on serine 51 [8]. The patient-derived EB virus-transformed lymphoblastoid cell line exhibited increased phosphorylation of eIF2α, suggesting increased ER stress (Fig. 4C).

4. Discussion

A splice acceptor mutation of *CD40LG* was identified in patient 1, and CD40LG expression was lower in this patient (Fig. 2B). This *CD40LG* mutation has previously been reported in hyper IgM syndrome (HIGM) [9], but neurodegeneration is not a common feature of HIGM disorder. We speculated that mutations in other genes were probably the cause of the atypical symptoms seen in our patient. A heterozygous non-frameshift deletion (c.1242_1244 del) in *POLG* (DNA polymerase subunit γ gene), which has not been described before, was identified as a candidate. *POLG* is essential for mitochondrial DNA (mtDNA) replication. Mutations in *POLG* have been identified in various diseases such as progressive external ophthalmoplegia (PEO), Alpers syndrome and other infantile hepatocerebral syndromes, ataxia-neuropathy syndromes, Charcot–Marie–Tooth disease, and idiopathic parkinsonism [10]. These diseases are characterized by mtDNA depletion in symptomatic tissues. Although a *POLG* in-frame nucleotide deletion was identified in patient 1, mtDNA levels were the same as in the other patients, suggesting that this in-frame nucleotide deletion does not interfere with POLG function (data not shown). This result suggests that the neurological symptoms in this patient are very unlikely to be modified by mutation of *POLG*.

Patients with CD40LG deficiency are susceptible to central nervous system (CNS) infections. The incidence of CNS infection or progressive neurodegeneration is 12–16% among patients with CD40LG deficiency [11]. Dysfunction of CD40–CD40LG dependent T-cell immunity attenuates $CD8^+$ T-cell trafficking to the CNS in mice, and this led to elevated West Nile virus titers and resulted in neurodegeneration [12]. Immunodeficiency caused by CD40LG deficiency can increase susceptibility to CNS infection, or allow persistent CNS infection, and this can explain the neurodegeneration observed in patients. Bishu et al. reported five patients exhibiting neurological symptoms, including ataxia, in a cohort of 31 patients. Although an infectious etiology is the most plausible explanation, no pathogens were identified in four of the patients with neurological symptoms. This group proposed that the lack of proof of infection necessitates consideration of other etiologies [13], which may also be the case with our patient. There are several interesting previous reports suggesting a relationship between CD40–CD40LG function and neuronal function. CD40LG is critical for protection from demyelinating disease and for development of spontaneous remyelination in a mouse model of multiple sclerosis produced by infection with Theiler's murine encephalomyelitis virus [14]. CD40–CD40LG interaction enables astrocytosis and microgliosis in response to amyloid-beta peptide [15]. Although CD40LG deficiency does not lead directly to neurodegeneration, CD40 is expressed and functional on mouse and human neurons. CD40-deficient mice display neuronal dysfunction, aberrant neuronal morphology, and associated gross brain abnormalities [16]. These findings suggest that an infection-based hypothesis is not the only possibility; changes in neuronal function could also explain the neurodegeneration seen as a result of CD40LG deficiency.

Mutation in *SIL1* causes MSS [17], an autosomal recessive disorder that is principally associated with cerebellar ataxia, bilateral cataracts, myopathy and mental retardation. The mutation seen in patient 5 in

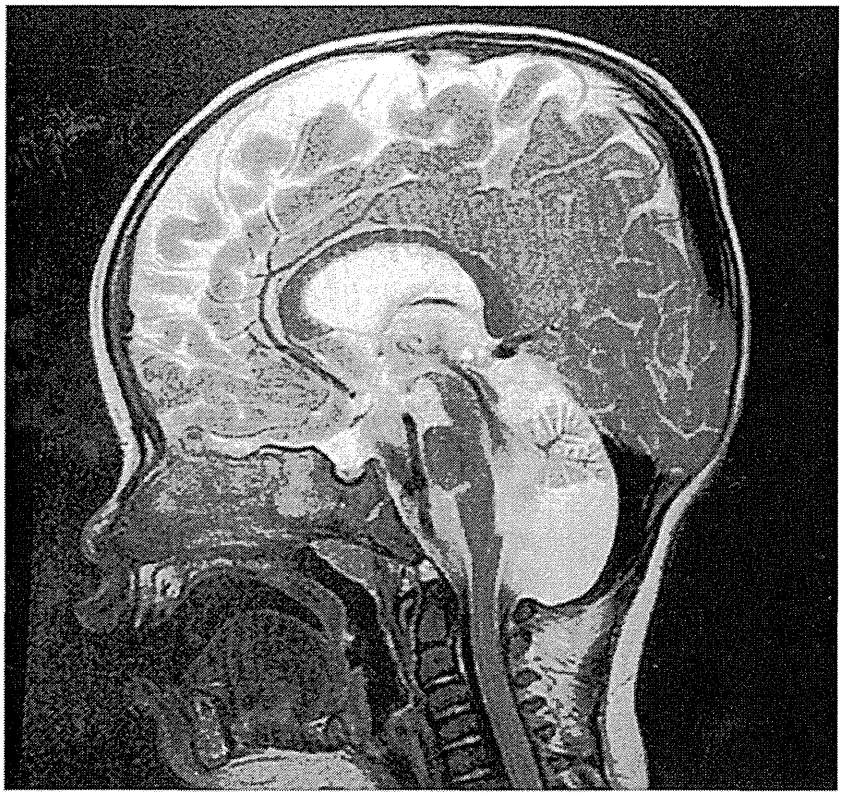

Fig. 3. Sagittal midline T2-weighted MR image of patient 5, demonstrating cerebellar atrophy of the vermis.

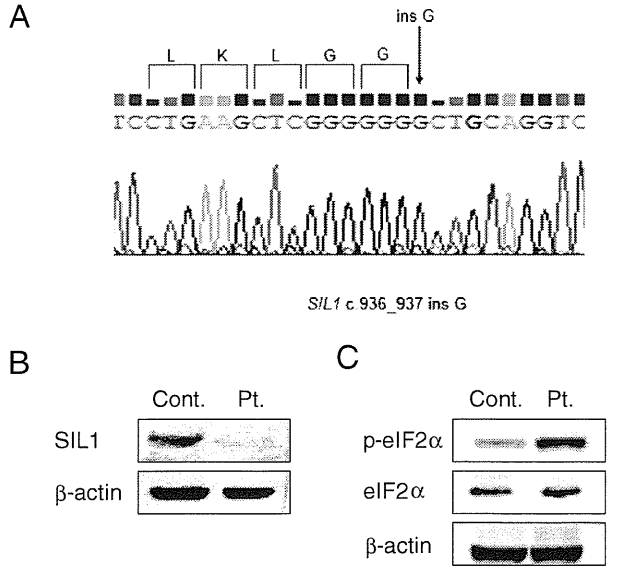

Fig. 4. A, Sequence electropherogram of *SIL1*. A homozygous frameshift mutation was identified. B, Western blotting analysis of SIL1 expression. C, eIF2α and phosphorylated eIF2α (p-eIF2α) levels. Cont: protein extract from EBV-transformed lymphoblastoid cell line derived from a healthy volunteer. Pt: protein extract from EBV-transformed lymphoblastoid cell line derived from patient 5.

this study was also reported in three unrelated Japanese patients with MSS [18]. Patient 5 did not demonstrate cataracts at 1 year of age, although cataracts are known to appear later in life [17]. Although hypogammaglobulinemia has not been previously described in MSS, patient 5 exhibited remarkably reduced levels of serum IgG_2 with a moderate decrease in total IgG and IgA levels. SIL1 functions in combination with BiP to ensure proper folding of proteins in the ER [7]. Assembly of the immunoglobulin heavy chain and light chain is performed in the ER in association with the ER chaperone, BiP [19]. In this study, we have not examined if hypogammaglobulinemia is a common feature of MSS or a specific feature of this case 5 patient. A further study of cases is therefore needed to reveal whether hypogammaglobulinemia is a common feature in MSS.

Several non-synonymous SNV, frameshift, or splice site mutations in DDR-associated genes were identified (Supplementary Table 1). Further studies are required to evaluate the functional effects of these SNVs.

Molecular genotypes are occasionally obscured by exogenous or endogenous factors, infections, treatments or the disease process. In addition, these factors can sometimes hinder the identification of causative mutations. Recent advances in genome analysis technology allow the identification of such mutations in subjects with indistinguishable phenotypes, and this can lead to an unpredictable molecular diagnosis for these patients. However, many of the well-known hereditary ataxias, including SCA, dentatorubral-pallidoluysian atrophy (DRPLA), and Friedreich's ataxia, are caused by tri-nucleotide expansions. In these cases, WES analysis may fail to identify the causative mutation. In fact, molecular diagnoses for the other seven patients in the present study remain elusive. A combination of copy number and WES analyses of family members may increase the sensitivity and accuracy of genetic diagnosis. WES analyses will help to diagnose cases in which symptoms have been altered by infections or concomitant multiple gene alterations.

Conflicts of interest

The authors declare that they have no conflicts of interest.

Acknowledgments

The authors would like to thank the patients and their families for sharing this information. This work was supported by Grants-in-Aid 'the Research on Measures for Intractable Diseases Project' from the Ministry of Health, Labor and Welfare of Japan (H23-012).

Appendix A. Supplementary data

Supplementary data to this article can be found online at http://dx.doi.org/10.1016/j.jns.2014.02.033.

References

[1] Shiloh Y. ATM and related protein kinases: safeguarding genome integrity. Nat Rev Cancer 2003;3(3):155–68.
[2] Gatti RA, Boder E, Good RA. Immunodeficiency, radiosensitivity, and the XCIND syndrome. Immunol Res 2007;38(1–3):87–101.
[3] Lavin MF, Gueven N, Grattan-Smith P. Defective responses to DNA single- and double-strand breaks in spinocerebellar ataxia. DNA Repair 2008;7(7):1061–76.
[4] Kunishima S, Okuno Y, Yoshida K, Shiraishi Y, Sanada M, Muramatsu H, et al. ACTN1 mutations cause congenital macrothrombocytopenia. Am J Hum Genet 2013;92(3):431–8.
[5] Tomizawa D, Aoki Y, Nagasawa M, Morio T, Kajiwara M, Sekine T, et al. Novel adopted immunotherapy for mixed chimerism after unrelated cord blood transplantation in Omenn syndrome. Eur J Haematol 2005;75(5):441–4.
[6] Buzin CH, Gatti RA, Nguyen VQ, Wen CY, Mitui M, Sanal O, et al. Comprehensive scanning of the ATM gene with DOVAM-S. Hum Mutat 2003;21(2):123–31.
[7] Van Raamsdonk JM. Loss of function mutations in SIL1 cause Marinesco–Sjogren syndrome. Clin Genet 2006;69(5):399–400.
[8] Donnelly N, Gorman AM, Gupta S, Samali A. The eIF2alpha kinases: their structures and functions. Cell Mol Life Sci 2013;70(19):3493–511.
[9] Lee WI, Torgerson TR, Schumacher MJ, Yel L, Zhu Q, Ochs HD. Molecular analysis of a large cohort of patients with the hyper immunoglobulin M (IgM) syndrome. Blood 2005;105(5):1881–90.
[10] Chan SS, Copeland WC. DNA polymerase gamma and mitochondrial disease: understanding the consequence of POLG mutations. Biochim Biophys Acta 2009;1787(5):312–9.
[11] Levy J, Espanol-Boren T, Thomas C, Fischer A, Tovo P, Bordigoni P, et al. Clinical spectrum of X-linked hyper-IgM syndrome. J Pediatr 1997;131(1 Pt 1):47–54.
[12] Sitati E, McCandless EE, Klein RS, Diamond MS. CD40–CD40 ligand interactions promote trafficking of CD8+ T cells into the brain and protection against West Nile virus encephalitis. J Virol 2007;81(18):9801–11.
[13] Bishu S, Madhavan D, Perez P, Civitello L, Liu S, Fessler M, et al. CD40 ligand deficiency: neurologic sequelae with radiographic correlation. Pediatr Neurol 2009;41(6):419–27.
[14] Drescher KM, Zoecklein LJ, Pavelko KD, Rivera-Quinones C, Hollenbaugh D, Rodriguez M. CD40L is critical for protection from demyelinating disease and development of spontaneous remyelination in a mouse model of multiple sclerosis. Brain Pathol 2000;10(1):1–15.
[15] Tan J, Town T, Crawford F, Mori T, DelleDonne A, Crescentini R, et al. Role of CD40 ligand in amyloidosis in transgenic Alzheimer's mice. Nat Neurosci 2002;5(12):1288–93.
[16] Hou H, Obregon D, Lou D, Ehrhart J, Fernandez F, Silver A, et al. Modulation of neuronal differentiation by CD40 isoforms. Biochem Biophys Res Commun 2008;369(2):641–7.
[17] Anttonen AK, Mahjneh I, Hamalainen RH, Lagier-Tourenne C, Kopra O, Waris L, et al. The gene disrupted in Marinesco–Sjogren syndrome encodes SIL1, an HSPA5 cochaperone. Nat Genet 2005;37(12):1309–11.
[18] Eriguchi M, Mizuta H, Kurohara K, Fujitake J, Kuroda Y. Identification of a new homozygous frameshift insertion mutation in the SIL1 gene in 3 Japanese patients with Marinesco–Sjogren syndrome. J Neurol Sci 2008;270(1–2):197–200.
[19] Lee YK, Brewer JW, Hellman R, Hendershot LM. BiP and immunoglobulin light chain cooperate to control the folding of heavy chain and ensure the fidelity of immunoglobulin assembly. Mol Biol Cell 1999;10(7):2209–19.

nature COMMUNICATIONS

ARTICLE

Received 7 Apr 2014 | Accepted 29 Apr 2014 | Published 4 Jun 2014

DOI: 10.1038/ncomms5004

Ulk1-mediated Atg5-independent macroautophagy mediates elimination of mitochondria from embryonic reticulocytes

Shinya Honda[1], Satoko Arakawa[1], Yuya Nishida[1], Hirofumi Yamaguchi[1], Eiichi Ishii[2] & Shigeomi Shimizu[1]

Macroautophagy is a highly conserved intracellular process responsible for the degradation of subcellular constituents. Macroautophagy was recently suggested to be involved in the removal of mitochondria from reticulocytes during the final stage of erythrocyte differentiation. Although Atg5 and Atg7 are indispensable for macroautophagy, their role in mitochondrial clearance remains controversial. We recently discovered that mammalian cells use conventional Atg5/Atg7-dependent macroautophagy as well as an alternative Unc-51-like kinase 1 (Ulk1)-dependent Atg5/Atg7-independent macroautophagy process. We hypothesized that the latter may be involved in mitochondrial clearance from reticulocytes during erythrocyte differentiation. Here we report that fetal definitive reticulocytes from Ulk1-deficient and Ulk1/Atg5 double-deficient mice retain their mitochondria, whereas the mitochondria are engulfed and digested within autophagic structures in wild-type and Atg5-deficient mice. Mitochondrial retention by Ulk1-deficient reticulocytes is far less marked in primitive and adult definitive reticulocytes. These data indicate that Ulk1-dependent Atg5-independent macroautophagy is the dominant process of mitochondrial clearance from fetal definitive reticulocytes.

[1] Department of Pathological Cell Biology, Medical Research Institute, Tokyo Medical and Dental University, 1-5-45 Yushima, Bunkyo-ku, Tokyo 113-8510, Japan. [2] Department of Pediatrics, Ehime University Graduate School of Medicine, Shitsukawa, Toon, Ehime 791-0295, Japan. Correspondence and requests for materials should be addressed to S.S. (email: shimizu.pcb@mri.tmd.ac.jp).

Macroautophagy is an essential maintenance and protective catabolic process involving the digestion of cellular components and damaged organelles within the lysosomes[1,2]. Macroautophagy occurs constitutively at a low level, but is accelerated by cellular stressors, such as starvation, lack of growth factors and DNA damage. The molecular basis of macroautophagy was extensively studied using autophagy-defective mutant yeasts and mammals[2,3]. It is currently accepted that macroautophagy is driven by >30 autophagy-related proteins (Atgs) conserved from yeasts to mammals[4]. The process of macroautophagy is initiated by the multiprotein complex phosphatidylinositol 3-kinase (PI3K) type III containing Atg6 (also called Beclin1), which promotes membrane invagination[5]. The subsequent elongation and closure of the isolation membrane is mediated by two ubiquitin-like conjugation pathways: the Atg5-Atg12 pathway and the microtubule-associated protein 1 light chain 3 (LC3) pathway[4]. Both pathways depend on the E1-like enzyme Atg7. Thus, several core macroautophagy molecules are believed to be indispensable for macroautophagy, particularly PI3K, Atg5 and Atg7.

We recently discovered that macroautophagy occurs in cells lacking Atg5 and Atg7 (ref. 6). We named this process 'alternative macroautophagy' to distinguish it from Atg5/Atg7-dependent conventional macroautophagy. The role is similar to conventional macroautophagy; whereby, cellular components and organelles are digested within autophagosomes. But the signalling pathway involves PI3K, and not Atg5, Atg7 or LC3. We also found that this pathway is largely dependent on Unc-51-like kinase 1 (Ulk1), a mammalian homologue of yeast Atg1. This kinase is involved in the initiation of conventional macroautophagy and several regulatory mechanisms have been proposed. During starvation, the mTOR complex 1 dissociates from Ulk1, leading to Ulk1 dephosphorylation and activation of the UlK1-Atg13-FIP200-Atg101 complex[7]. In another pathway, Ulk1 is stabilized and activated by the Hsp90-Cdc37 complex[8]. Furthermore, it has been reported that Ulk1 is phosphorylated and acetylated by AMP-activated protein kinase (AMPK)[9] and Tip60 (ref. 10), respectively. All of the above reports were related to the mechanisms by which Ulk1 initiates conventional macroautophagy. However, cells from Ulk1-knockout mice maintained low but significant macroautophagy activity[11]. This study suggests that Ulk1 is not essential for conventional Atg5/Atg7-dependent macroautophagy, but improves the efficiency[11]. This kinase was upregulated during alternative macroautophagy, and Ulk1 silencing markedly inhibited the alternative process[6]. Therefore, Ulk1 may have a dual role, as a facilitator of conventional macroautophagy and as an essential trigger for alternative macroautophagy.

Macroautophagy was previously considered to be a nonselective process, but recent studies demonstrated that distinct macroautophagy signalling pathways regulate the digestion of specific organelles[12,13]. During erythrocyte maturation,

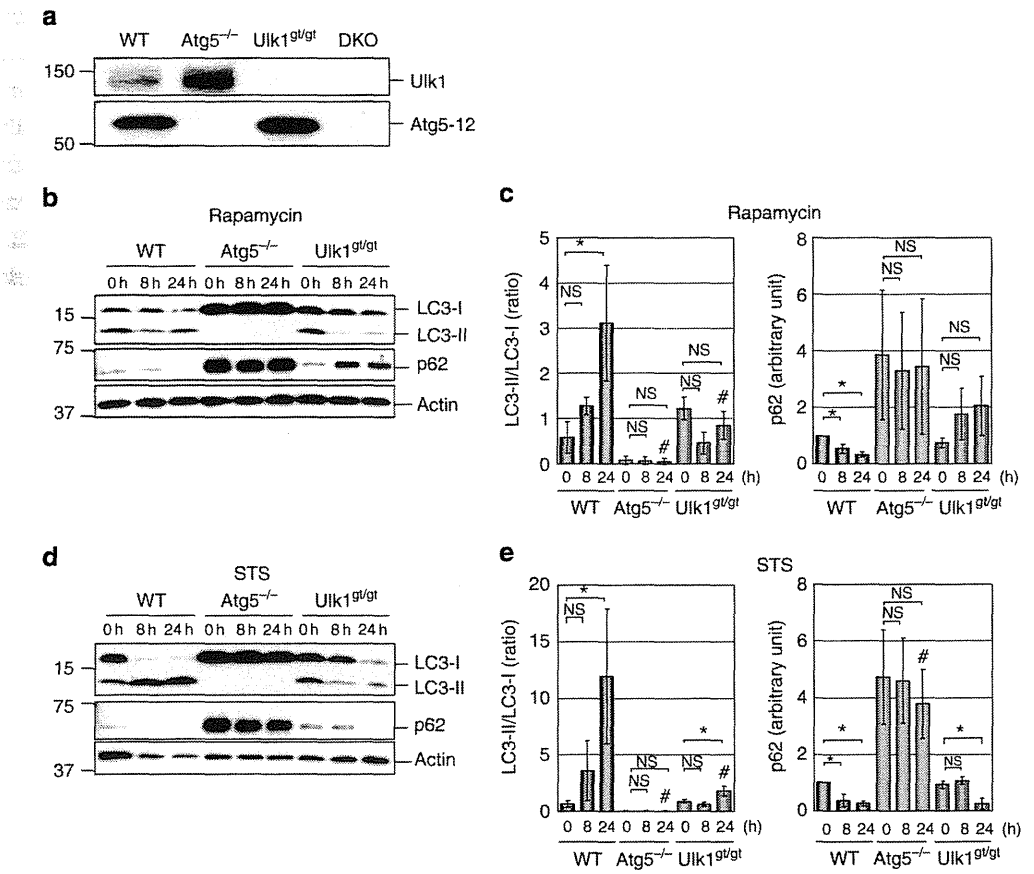

Figure 1 | Induction of conventional macroautophagy in Atg5-deficient erythroid cells by rapamycin and STS. (**a**) Expression of Ulk1 and Atg5-12 in the indicated erythroid cells. (**b–e**) Induction of conventional macroautophagy in WT and $Ulk1^{gt/gt}$, but not in $Atg5^{-/-}$, embryonic erythroid cells. $Ter119^{+}$ erythroid cells from WT, $Atg5^{-/-}$, and $Ulk1^{gt/gt}$ embryonic mice (E18.5) were treated with 1 μM rapamycin (**b**,**c**) and 1 μM STS (**d**,**e**), and then harvested at the indicated times. (**b**,**d**) Representative protein expression of LC3 and p62 measured by western blot. Actin was a loading control. Uncropped images are shown in Supplementary Fig. 10. (**c**,**e**) Semi-quantitative analysis of LC3-II/LC3-I and p62 protein expression ($n=3$, mean ± s.d.). Asterisks indicate a significant difference at $P<0.05$ (analysis of variance (ANOVA)). $^{\#}P<0.05$ versus value of WT 24 h (ANOVA). 'NS' indicates not significant (ANOVA).

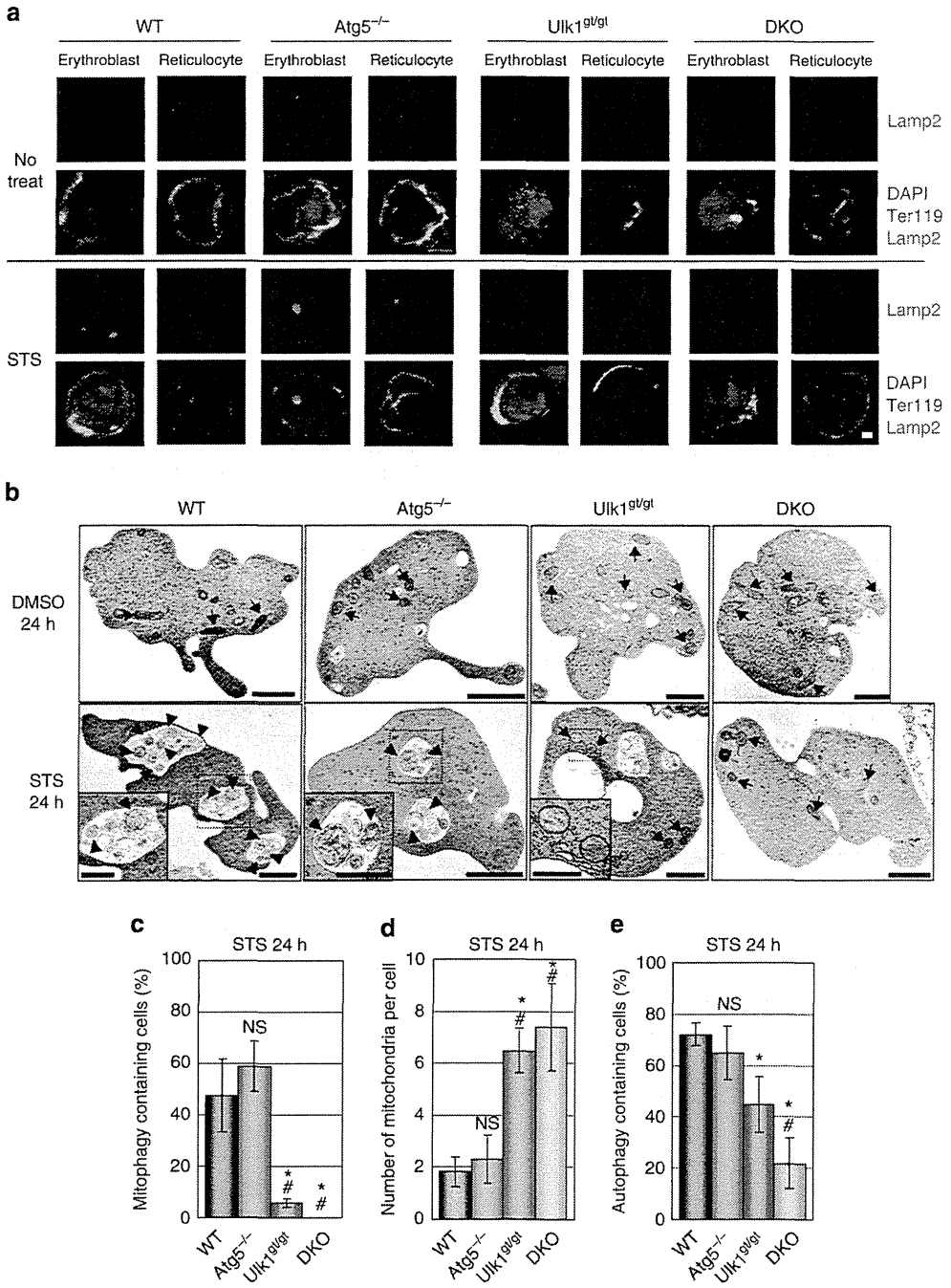

Figure 2 | Induction of alternative macroautophagy in Atg5-deficient erythroid cells by STS. (**a**) Induction of alternative macroautophagy in WT and Atg5$^{-/-}$, but not Ulk1$^{gt/gt}$ and DKO, erythroid cells. Erythroblasts and reticulocytes from the liver of embryonic mice (E18.5) were incubated with or without STS (1 μM) for 24 h, followed by staining with anti-Lamp2 (red), anti-Ter119 (green) and DAPI (blue). DAPI-positive erythroblasts and DAPI-negative reticulocytes are shown. Lamp2 image and merged image (DAPI, Ter119 and Lamp2) are shown. Scale bar, 1 μm. Large dots for Lamp2 are observed in STS-treated WT and Atg5$^{-/-}$ cells, but not STS-treated Ulk1$^{gt/gt}$ or DKO cells. (**b**) Representative electron micrographs of EC incubated with or without STS. Erythroid cells were harvested from the liver of embryonic mice (E18.5), incubated with or without STS (1 μM) for 24 h, and analysed by electron microscopy (EM). Scale bar, 1 μm. Insets of WT and Atg5$^{-/-}$ cells show mitophagy (Scale bar, 0.5 μm). Inset of a Ulk1$^{gt/gt}$ cell showing mitochondria that have not been engulfed (Scale bar, 0.5 μm). Arrows point to non-engulfed mitochondria and the arrowheads indicate engulfed mitochondria. (**c–e**) Quantitative analysis of mitophagy after STS treatment, calculated from EM photos. Population of reticulocytes with mitophagy (**c**), number of mitochondria per reticulocytes (**d**) and population of reticulocytes showing macroautophagy (**e**) were calculated ($n>35$ cells per mouse). The data are shown as mean ± s.d. ($n=3$). $^{*}P<0.05$ versus value of WT (analysis of variance (ANOVA)); $^{\#}P<0.05$ versus value of Atg5$^{-/-}$ (ANOVA); 'NS' indicates not significant versus value of WT (ANOVA).

the erythroblasts lose their nuclei to become reticulocytes, which are transformed into erythrocytes (EC) by the elimination of organelles, including the mitochondria. It is believed that macroautophagy is involved in this process because ultrastructural studies have detected autophagic structures engulfing mitochondria[14,15]. The involvement of Atg5 and Atg7 remains controversial due to conflicting reports[16–18]. In contrast, Ulk1 has been reported to have an important role[8,11]. Therefore,

we hypothesized that mitochondrial clearance during erythrocyte maturation may be performed by Ulk1-dependent Atg5-independent alternative macroautophagy. This hypothesis was tested by studying mitochondrial clearance from fetal definitive reticulocytes from Ulk1-deficient, Atg5-deficient and Ulk1/Atg5 double-deficient mouse embryos. The contribution of alternative macroautophagy was determined on the basis of the difference between the Atg5-deficient embryos and Ulk1/Atg5 double-deficient embryos. We also determined the weak involvement of Ulk1 in mitochondrial clearance from primitive and adult definitive reticulocytes. Our findings indicate that Ulk1-dependent Atg5-independent macroautophagy is the dominant pathway for mitochondrial clearance from fetal definitive reticulocytes, whereas its role is less important in primitive and adult definitive reticulocytes.

Results

Generation of Ulk1-deficient and Atg5/Ulk1-deficient mice. Ulk1-deficient mice were generated from embryonic stem cells by inserting a gene-trap in *ulk1* (Supplementary Fig. 1a). The absence of Ulk1 protein in the hematopoietic cells of $Ulk1^{gt/gt}$ mice was verified by western blotting (Fig. 1a). The $Ulk1^{gt/gt}$ mice showed mild anaemia (Supplementary Fig. 1b) and splenomegaly (Supplementary Fig. 1c), consistent with the phenotype of $Ulk1^{-/-}$ mice[11]. In addition, Ulk1/Atg5 double-deficient (DKO) mice were generated by crossbreeding $Ulk1^{gt/gt}$ mice with $Atg5^{+/-}$ mice (Fig. 1a). The terminal differentiation of EC proceeded normally in $Ulk1^{gt/gt}$, $Atg5^{-/-}$ and DKO mice, as assessed by the expression of Ter119 and CD71 (Supplementary Fig. 2). These markers were used to identify the different maturation stages of erythroid cells into EC.

Induction of Ulk1-dependent mitophagy by staurosporine. The wild-type (WT), $Ulk1^{gt/gt}$ and $Atg5^{-/-}$ mice were first tested for the presence of functional conventional and/or alternative macroautophagy in cells of the erythroid lineage. The cells were harvested from the liver of embryonic mice on day 18.5 (E18.5) using microbeads conjugated with anti-Ter119 antibodies. The cells were treated with rapamycin to selectively induce conventional (not alternative) macroautophagy[6], and examined for the lipid conjugation of microtubule-associated protein LC3 that occurs during conventional (but not alternative) macroautophagy[6]. LC3-II (a lipid conjugate) was observed in WT cells, but not in $Atg5^{-/-}$ cells, after rapamycin treatment (Fig. 1b,c). Lesser LC3-II formation was detected in $Ulk1^{gt/gt}$ cells than in WT. We also examined the expression of p62, a specific substrate of conventional macroautophagy. Consistent with LC3-II formation, the highest expression of p62 was found in $Atg5^{-/-}$ cells, followed by $Ulk1^{gt/gt}$ and WT cells (Fig. 1b,c). Similar results were obtained when these cells were treated with staurosporine (STS), a pan-kinase inhibitor (Fig. 1d,e). These results show that the lack of Ulk1 expression partially inhibited conventional macroautophagy in erythroid cells.

Conventional and alternative macroautophagy were visualized by confocal microscopy using the non-selective autophagy inducer STS and antibodies against lysosomal-associated membrane protein 2 (Lamp2). Lysosomes are small vesicles distributed throughout the cytosol, so that Lamp2 fluorescence is seen as tiny dots. After the induction of macroautophagy, lysosomes fuse with autophagic vacuoles and the area of Lamp2 fluorescence become much larger. Thus, large Lamp2 fluorescence dots are identical to autolysosomes, as described previously[6]. Small diffuse fluorescent dots were observed in untreated WT erythroid cells, whereas STS-treated WT erythroid cells contained large fluorescent dots (Fig. 2a) suggestive of macroautophagy induction. Large fluorescent dots similar in size and number were observed in STS-treated $Atg5^{-/-}$ erythroid cells. Because conventional macroautophagy was not induced in these cells, the large Lamp2 dots suggest that STS induced alternative macroautophagy. In contrast, fewer large Lamp2 dots were detected in STS-treated $Ulk1^{gt/gt}$ and STS-treated $Ulk1^{gt/gt}$ $Atg5^{-/-}$ DKO erythroid cells, suggesting that Ulk1 is involved in both conventional and alternative macroautophagy.

The two types of macroautophagy were distinguished using anti-LC3 antibodies because this protein only associates with autolysosomes during conventional macroautophagy, and therefore is a good marker to distinguish these two types of autophagic machineries. In this assay, the addition of a lysosomal protease inhibitor (E64d) was required to prevent LC3 degradation in autolysosomes. Selective induction of conventional macroautophagy with rapamycin generated only LC3-positive Lamp2 dots in WT cells (Supplementary Fig. 3). In contrast, STS-treated $Atg5^{-/-}$ cells, where alternative macroautophagy was selectively generated, contained only LC3-negative Lamp2 dots (Supplementary Fig. 3). Expectedly, STS-treated WT and $Ulk1^{gt/gt}$ cells possessed both types of Lamp2 dots. In addition, the size and number of Lamp2 dots was significantly lower in $Ulk1^{gt/gt}$ cells (Supplementary Fig. 3). These findings suggest that STS induces conventional and alternative macroautophagy, both of which are largely dependent on Ulk1.

Figure 3 | Impaired clearance of mitochondria in $Ulk1^{gt/gt}$ and DKO EC. (**a**) Three-colour flow cytometry of erythroid cells from WT embryonic liver (E14.5) stained with anti-Ter119, anti-CD71 and Mitotracker Deep Red. (Left upper panel) Ter119 versus CD71 fluorescence. (Other panels) FSC versus Mitotracker fluorescence of the R1 (right upper panel), R2 (left lower panel) and R3 (right lower panel) fractions. (**b**,**c**) Percentage of cells with a low number of mitochondria (mitochondria^{low} cells) among $CD71^-Ter119^+$ EC. Erythroid cells from the liver (E14.5 and E18.5) and peripheral blood (E18.5) of indicated mice were stained with anti-Ter119, anti-CD71 and Mitotracker Deep Red. (**b**) Representative histograms of mitochondrial content in $CD71^-Ter119^+$ cells. Numbers indicate the population of mitochondria^{low} cells. (**c**) The percentage of $CD71^-Ter119^+$ cells without mitochondria was determined by gating the mitochondria^{low} fraction, as shown in (**b**) (mean ± s.d., $n=6$). $^*P<0.05$ versus value of WT (analysis of variance (ANOVA)); $^{\#}P<0.05$ versus value of $Atg5^{-/-}$ (ANOVA); 'NS' indicates not significant versus value of WT (ANOVA). (**d**) Percent mitochondria^{low} cells in the $CD71^-Ter119^+$ EC of $Atg7^{F/F}$Cre embryo. Erythroid cells from the liver and peripheral blood of WT and $Atg7^{F/F}$Cre embryo (E18.5) were stained with anti-Ter119, anti-CD71, and Mitotracker Deep Red (mean ± s.d., $n=3$). $^*P<0.05$ versus value of WT (Student's *t*-test). (**e**) Percentage of mitochondria^{low} cells in Syto16^{low} cells. Liver erythroid cells (E18.5) were stained with Syto16 (DNA) and Mitotracker Deep Red. Representative dot plots of the mitochondrial content of Syto16^{low} cells are demonstrated in Supplementary Fig. 5, the percentage of Syto16^{low} cells without mitochondria was determined by gating the mitochondria^{low} fraction (mean ± s.d., $n=6$). $^*P<0.05$ versus value of WT (ANOVA); $^{\#}P<0.05$ versus value of $Atg5^{-/-}$ (ANOVA); 'NS' indicates not significant versus value of WT (ANOVA). (**f**) Immunofluorescent analysis of mitochondrial and lysosomal proteins. Liver $Ter119^+$ cells (E18.5) of the indicated mice were stained with anti-Tom20 (mitochondrial marker) and anti-Lamp2 (lysosomal marker) antibodies, and observed by fluorescent microscopy. Scale bar, 2 μm. Green, red, white, and blue indicate Tom20, Lamp2, Ter119 and DAPI (DNA), respectively. Mitochondrial and lysosomal markers have separate distributions in $Ulk1^{gt/gt}$ cells and DKO cells.

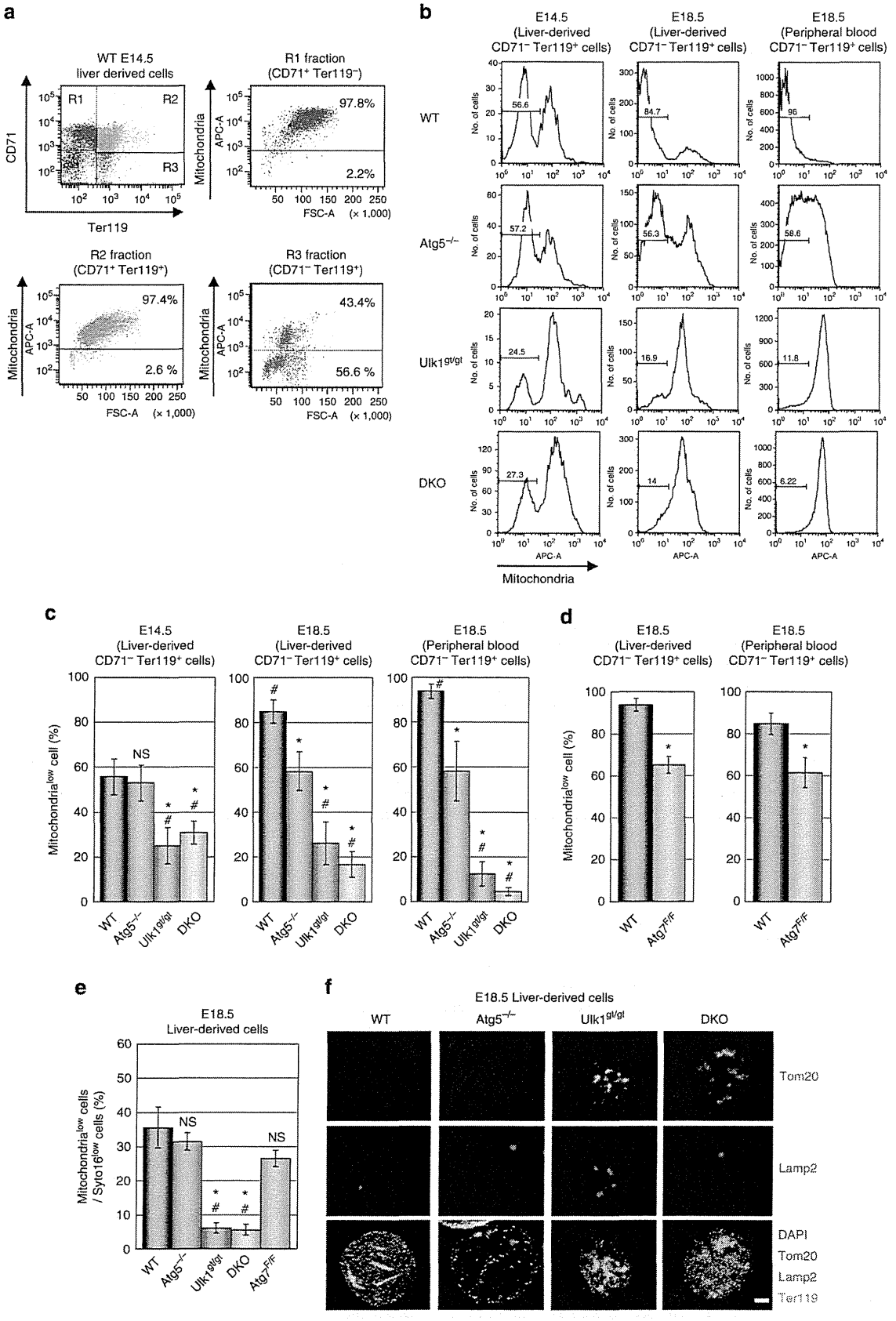

The process of STS-mediated macroautophagy in erythroid cells was further examined by electron microscopy. In WT cells, this exposure caused the formation of several large autophagic vacuoles. The vacuoles engulfed cytoplasmic constituents and mitochondria. Erythroid cells may be unusually susceptible to mitochondrial digestion by macroautophagy ('mitophagy') because this phenomenon was rarely observed in STS-treated embryonic fibroblasts. Similar autophagic vacuoles were observed

in Atg5$^{-/-}$ erythroid cells, but not in DKO erythroid cells (Fig. 2b). Quantitative analysis revealed that mitophagy occurred in about 50% of WT cells and 60% of Atg5$^{-/-}$ cells (Fig. 2c), and the number of mitochondria among these cells was low (Fig. 2d). Autophagic vacuoles were also observed in STS-treated Ulk1$^{gt/gt}$ cells (Fig. 2b,e), but most of them were not used for mitophagy. Thus, the cell population exhibiting mitophagy was small (Fig. 2c), and the number of mitochondria in STS-treated Ulk1$^{gt/gt}$ cells was higher than in STS-treated WT or STS-treated Atg5$^{-/-}$ cells (Fig. 2d). DKO cells contained only a few autophagic vacuoles (Fig. 2b,e), and the mitochondrial numbers were high (Fig. 2d). Although STS is a well-known apoptosis inducer, the apoptotic cell population was low (<25%) under these conditions (Supplementary Fig. 4a). Furthermore, the apoptosis inhibitor Qvd-fmk did not significantly alter the extent of mitochondrial clearance (Supplementary Fig. 4b), indicating that apoptosis was not involved in macroautophagy and mitochondrial clearance. Altogether, these findings indicate that STS induces both conventional and Ulk1-dependent alternative macroautophagy in erythroid cells, and that mitochondria are mainly removed by the latter.

Mitochondrial removal by alternative macroautophagy *in vivo*. Experiments were designed to determine the role of Ulk1-dependent alternative macroautophagy in mitochondrial clearance during erythrocyte differentiation. Hematopoietic ontogeny includes three waves of erythroid lineage: primitive, fetal definitive and adult definitive. The existence of this process in fetal definitive erythroid cells was assessed. Three-colour flow cytometric analysis was conducted using a marker of erythroid precursors (CD71), a marker of late stage erythroid lineage (Ter119) and mitochondria-specific Mitotracker Deep Red staining, indicating that nearly all CD71^{+}Ter119^{-} cells (Fig. 3a left upper panel; R1 fraction) and CD71^{+}Ter119^{+} cells (Fig. 3a left upper panel; R2 fraction) showed strong Mitotracker staining (Fig. 3a right upper and left lower panels) in erythroid cells harvested from the liver of WT embryos on E14.5. In contrast, about 60% of the CD71^{-}Ter119^{+} cells (mature EC) showed weak Mitotracker staining (Fig. 3a left upper panel; R3 fraction, Fig. 3a right lower panel) due to mitochondrial clearance during differentiation. The cell population containing low numbers of mitochondria (mitochondria^{low} cells) among mature Atg5$^{-/-}$ EC (Fig. 3b,c; E14.5 Atg5$^{-/-}$) was equivalent to that of mature WT EC (Fig. 3b,c; E14.5 WT). This population was smaller in Ulk1$^{gt/gt}$ and DKO EC (Fig. 3b,c; E14.5 Ulk1$^{gt/gt}$ and DKO). These data show that erythrocyte differentiation requires Ulk1, but not Atg5, for mitochondrial clearance on E14.5.

In mature EC harvested from the liver and blood on E18.5, most WT cells no longer contained mitochondria (Fig. 3b,c; E18.5 WT), whereas <25% of Ulk1$^{gt/gt}$ and DKO EC had lost their mitochondria (Fig. 3b,c; E18.5 Ulk1$^{gt/gt}$ and DKO), indicating a failure to clear mitochondria in the absence of Ulk1. The mitochondria^{low} population among mature Atg5$^{-/-}$ EC was smaller than that among mature WT EC, but considerably larger than that among Ulk1$^{gt/gt}$ and DKO EC (Fig. 3b,c; E18.5 Atg5$^{-/-}$). Similar results were obtained with hematopoietic-specific Atg7 conditional knockout (Atg7$^{F/F}$;vav1-cre (Atg7$^{F/F}$Cre)) mice (Fig. 3d). These data indicate that Ulk1 plays a predominant role, compared with that of Atg5 and Atg7, in mitochondrial clearance from reticulocytes on E18.5. During erythrocyte differentiation, mitochondria elimination is initiated after enucleation. Therefore, the efficiency of mitochondrial clearance was determined by staining cells with the DNA-specific stain Syto16 and Mitotracker Deep Red. Syto16^{low} cells identified enucleated cells, and the efficiency was calculated from the ratio of mitochondria^{low} Syto16^{low} cells to the total amount of Syto16^{low} cells (Supplementary Fig. 5). The population of mitochondria^{low} Syto16^{low} EC was smaller in Ulk1$^{gt/gt}$ and DKO embryos than in WT, Atg5$^{-/-}$ and Atg7$^{F/F}$Cre embryos (Fig. 3e). These data are consistent with the results obtained by Ter119/CD71/Mitotracker staining (Fig. 3c,d). Furthermore, when late erythroid lineage Ter119-positive cells were immunostained with mitochondria-specific anti-Tom20 antibodies, positive signals were detected in most Ulk1$^{gt/gt}$ and DKO EC, but only in a few WT and Atg5$^{-/-}$ EC (Fig. 3f). Mitochondrial signals rarely merged with Lamp2 fluorescence in Ulk1$^{gt/gt}$ and DKO EC, suggesting that mitophagy did not occur. Altogether, these data indicate that Ulk1 is considerably more important than Atg5 for mitochondrial clearance from reticulocytes during the embryonic period.

The involvement of macroautophagy during the mitochondrial clearance from reticulocytes was further investigated on the basis of ultrastructural changes visualized by EM. On E14.5, the mitochondria was engulfed and digested by autophagic vacuoles in WT reticulocytes (Fig. 4a) and Atg5$^{-/-}$ reticulocytes (Fig. 4b). The cell population exhibiting mitophagy was similar in these two types of reticulocytes (Fig. 4g), whereas mitophagy was largely suppressed in Ulk1$^{gt/gt}$ reticulocytes (Fig. 4c,g). These findings are consistent with the data obtained by flow cytometry (Fig. 3c,e). In DKO reticulocytes, mitophagy was also markedly suppressed, compared with WT reticulocytes (Fig. 4e,g). Accordingly, the number of mitochondria remaining in Ulk1$^{gt/gt}$ and DKO reticulocytes was larger than in WT and Atg5$^{-/-}$ reticulocytes (Fig. 4h). Numerous mitochondria were in contact with the membranous structure in Ulk1$^{gt/gt}$ and DKO reticulocytes. This may indicate that mitochondria were recognized by the isolation membrane, but not enclosed due to the lack of Ulk1. Some of the Ulk1$^{gt/gt}$ and DKO reticulocytes formed plasma membrane blebs and shed cell fragments containing mitochondria (Fig. 4d,f), which may represent a process that removes undigested mitochondria. All these morphological findings support a predominant role for Ulk1-dependent Atg5-independent macroautophagy in the mitochondrial clearance from reticulocytes.

To address the molecular mechanisms of mitophagy during erythrocyte differentiation, erythroblasts (EB; mitochondria^{high} Syto16^{high} cells) and reticulocytes (RC; mitochondria^{high} Syto16^{low} cells) were isolated from embryonic liver using Ter119-conjugated beads, followed by flow cytometric cell sorting. EC (Ter119-positive cells) were also purified from peripheral blood using Ter119-conjugated beads. The expression of key mitochondrial proteins was examined by western blotting. The mitochondrial outer membrane proteins, Tom20 and VDAC, were absent in EC from WT embryos due to mitochondrial clearance. They were detected at low levels in Atg5$^{-/-}$ EC and at high levels in Ulk1$^{gt/gt}$ and DKO EC (Fig. 5a,b). These data confirmed the partial impairment of mitochondrial clearance in Atg5$^{-/-}$ and severe impairment in Ulk1$^{gt/gt}$ and DKO EC. The protein Nix was recently identified as a selective autophagy receptor responsible for mitochondrial clearance from reticulocytes[19–22]. Accordingly, the expression level of Nix in these cell types was proportional to the extent of mitophagy (Fig. 5a,b; EC). Conventional macroautophagy was detected in WT and Ulk1$^{gt/gt}$, but not in Atg5$^{-/-}$ and DKO, erythroblasts and reticulocytes, based on the levels of LC3-II and p62 (Fig. 5a,b). However, this process may not be involved in mitochondrial clearance because mitophagy occurred in Atg5$^{-/-}$ cells where conventional macroautophagy was absent. Furthermore, most signals for LC3 (conventional macroautophagy marker) did not co-localize with Tom20 signals (mitochondria marker) in the erythroblasts and early reticulocytes of WT and Ulk1$^{gt/gt}$ embryos (Supplementary Fig. 6). Therefore, conventional macroautophagy

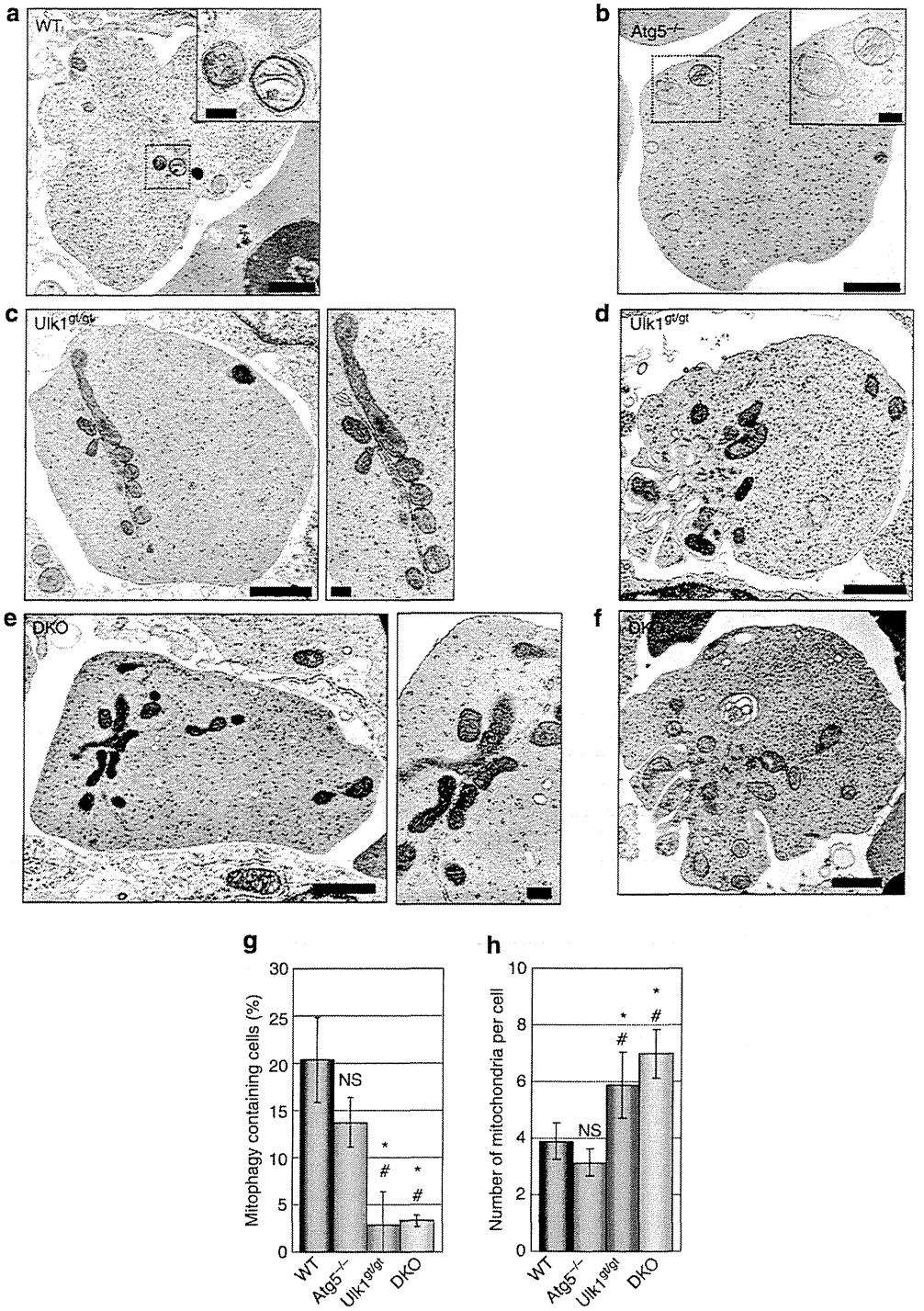

Figure 4 | Clearance of mitochondria by macroautophagy from reticulocytes of WT and Atg5$^{-/-}$ mice, but not Ulk1$^{gt/gt}$ or DKO mice. (**a**–**f**) Representative EM of WT (**a**), ATG5$^{-/-}$ (**b**), Ulk1$^{gt/gt}$ (**c**,**d**) and DKO (**e**,**f**) reticulocytes from embryonic liver (E14.5). (**a**,**b**) Mitophagy was detected in WT and ATG5$^{-/-}$ cells (scale bar, 1 μm). Insets indicate mitophagy (scale bar, 0.2 μm). (**c**,**e**) In Ulk1$^{gt/gt}$ and DKO cells, numerous mitochondria were in contact with membrane structures (scale bar, 1 μm). Enlarged images are shown on the right side (scale bar, 0.2 μm). (**d**,**f**) Some Ulk1$^{gt/gt}$ and DKO cells showed plasma membrane blebs containing mitochondria (scale bar, 1 μm). (**g**,**h**) Quantitative analysis of mitophagy calculated from EM photos in the embryonic liver at E18.5. Population of reticulocytes with mitophagy (**g**), and number of mitochondria per reticulocytes (**h**) were calculated ($n>35$ cells per mouse). The data are shown as mean ± s.d. ($n=3$). $^{*}P<0.05$ versus value of WT (analysis of variance (ANOVA)); $^{\#}P<0.05$ versus value of Atg5$^{-/-}$ (ANOVA); 'NS' indicates not significant versus value of WT (ANOVA).

would not contribute to mitochondrial clearance from fetal definitive reticulocytes.

The WT and Atg5$^{-/-}$ reticulocytes expressed a high molecular weight Ulk1 isoform, compared with their erythroblasts (Fig. 5a). Ulk1 is regulated by posttranslational modifications such as phosphorylation[8,9] and acetylation[10]. Since the Ulk1 modification in reticulocytes was not changed by phosphatase treatment (Fig. 5c), Ulk1 acetylation, but not phosphorylation, seems to be crucial for mitochondrial clearance, although the possibility was not excluded that unidentified

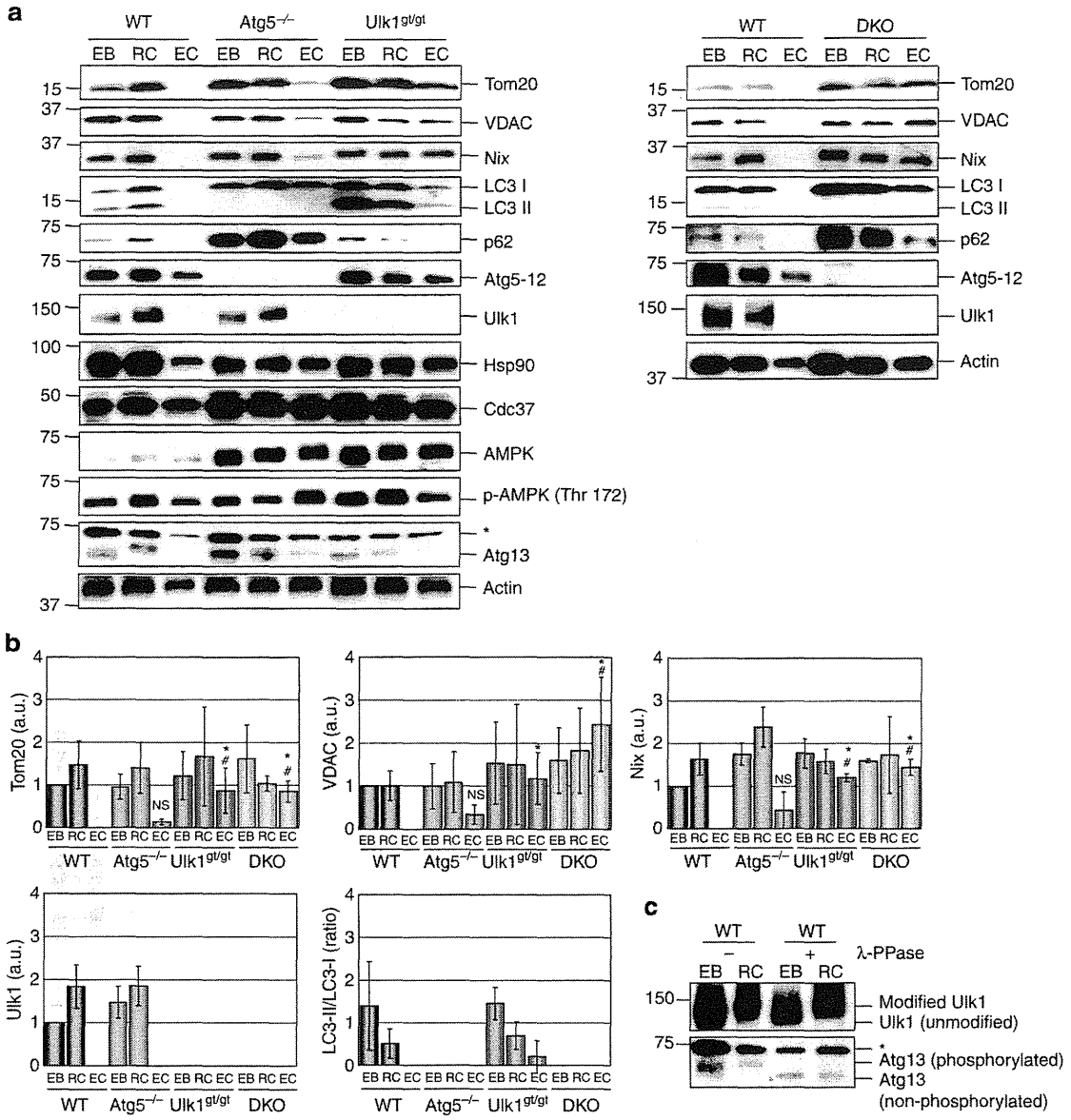

Figure 5 | Expression of autophagy-related proteins during erythrocyte differentiation. (**a**) Erythroblasts (EB; mitochondria^{high} Syto16^{high}), reticulocytes (RC; mitochondria^{high} Syto16^{low}) and EC (EC; Ter119^{+} PBC) were collected from the indicated embryos (E18.5), and the expression of each protein was examined by western blot. The asterisk indicates a nonspecific band. Uncropped images are shown in Supplementary Figs 11 and 12. (**b**) Semi-quantitative analysis of the expression level of each protein and the LC3-II/LC3-I ratio (mean ± s.d., $n=3$). $^{*}P<0.05$ versus value of WT EC (analysis of variance (ANOVA)); $^{\#}P<0.05$ versus value of Atg5$^{-/-}$ EC (ANOVA); 'NS' indicates not significant versus value of WT EC (ANOVA). (**c**) Modification of Ulk1 and Atg13 during erythrocyte maturation. Cell lysates were treated with λ-phosphatase (400 U) for 45 min at 30 °C, and band shift was examined by anti-Ulk1 and anti-Atg13 antibodies. Asterisk indicates non-specific band. Uncropped images are shown in Supplementary Fig. 12.

modification occurs in Ulk1. Although Hsp90, Cdc37 and AMPK were recently found responsible for Ulk1 activation[8,9], these proteins were slightly upregulated in WT reticulocytes, but not in Atg5$^{-/-}$ reticulocytes (Fig. 5a) despite the occurrence of mitophagy. In addition, a downstream effector of Ulk1 (Atg13) may be phosphorylated in WT reticulocytes (based on phosphatase reaction (Fig. 5c)), but not in Atg5$^{-/-}$ reticulocytes (Fig. 5a). These data support the existence of an unidentified Ulk1-mediated signalling pathway promoting cell differentiation in Atg5$^{-/-}$ reticulocytes.

Mitochondrial removal by alternative macroautophagy *in vitro*. The involvement of alternative macroautophagy in mitochondrial clearance during erythrocyte maturation was further confirmed using an *in vitro* erythrocyte differentiation system. Nascent erythroblasts were purified from the liver of E14.5 embryos and cultured in erythrocyte differentiation medium (see Methods). Three days after the induction of differentiation, >60% of the cells had lost their nuclei and become reticulocytes in every genotype (Fig. 6a,b). Thereafter, the enucleated cells (Syto16^{low} cells) lost their mitochondria in the cultures of WT cells, as shown by a gradual increase in the number of mitochondria^{low} Syto16^{low} cells (mature red blood cells) (Fig. 6c,d). Similar results were obtained with Atg5$^{-/-}$ erythroid cells. In contrast, the number of mitochondria^{low} Syto16^{low} cells did not increase in Ulk1$^{gt/gt}$ and DKO cells (Fig. 6c,d), indicating that Ulk1 is essential for mitochondrial clearance during *in vitro* differentiation, which is consistent with the *in vivo* findings. Wortmannin and 3-methyladenine are frequently used autophagy inhibitors known to inhibit both conventional and alternative